KANSAS GEOLOGICAL SURVEY
OPEN-FILE REPORT 2003-72

SEISMIC INVESTIGATION OF A SINKHOLE ON CLEARWATER DAM

by

Richard D. Miller
Julian Ivanov
David R. Laflen
Joe M. Anderson

Disclaimer

The Kansas Geological Survey does not guarantee this document to be free from errors or inaccuracies and disclaims any responsibility or liability for interpretations based on data used in the production of this document or decisions based thereon. This report is intended to make results of research available at the earliest possible date, but is not intended to constitute final or formal publications.

Kansas Geological Survey
1930 Constant Avenue
University of Kansas
Lawrence, KS 66047-3726

Surface Seismic Investigation of a Sinkhole on Clearwater Dam, Missouri

Richard D. Miller
Julian Ivanov
David R. Laflen
Joe M. Anderson
Mary C. Brohammer

Kansas Geological Survey
1930 Constant Avenue
Lawrence, Kansas 66047

Final Report to

Steve Hartung
Little Rock District, U.S. Army Corps of Engineers
700 West Capitol
Little Rock, Arkansas 77203-0867

Open-file Report 2003-72

June 24, 2004

The Kansas Geological Survey makes no warranty or representation, either express or implied, with regard to the data, documentation, or interpretations or decisions based on the use of this data including the quality, performance, merchantability, or fitness for a particular purpose. Under no circumstances shall the Kansas Geological Survey be liable for any damages of any kind, including direct, indirect, special, incidental, punitive, or consequential damages in connection with or arising out of the existence, furnishing, failure to furnish, or use of or inability to use any of the data or documentation whether as a result of contract, negligence, strict liability, or otherwise.

Surface Seismic Investigation of a Sinkhole on Clearwater Dam, Missouri

by
Richard D. Miller
Julian M. Ivanov
David R. Laflen
Joe M. Anderson
Mary C. Brohammer

Kansas Geological Survey
University of Kansas Center for Research, Inc.
1930 Constant Avenue, Campus West
Lawrence, Kansas 66047-3726

Final Report to

Steve Hartung
Little Rock District, U.S. Army Corps of Engineers
700 West Capitol
Little Rock, Arkansas 72203-0867

June 24, 2004

Open-file Report No. 2003-72

Surface Seismic Investigation of a Sinkhole on Clearwater Dam, Missouri

Summary

A sinkhole that formed on Clearwater Dam during January of 2003 was the target of a high-resolution seismic imaging program that included both seismic reflection and surface wave analysis. The primary goal of this surface seismic investigation was to determine the general subsidence geometry within the dam (the "root or chimney" of the sinkhole) and help ascertain if and to what extent bedrock and native alluvium were involved with the sinkhole. This sinkhole formed approximately 120 ft on the upstream side of the dam crest and when first discovered measured 10 ft across and 10 ft deep. Seismic data provide insights into the areal extent and approximate affected volume of dam material. Based on seismic, construction, drill, and bore-hole tracer data, a borehole geophysics program was designed to identify fractures/joints that might provide pathways for upstream water to flow through the pervious fill material and leak past the impervious core. A comprehensive appraisal of the risk this disturbed zone represents to the overall integrity of the dam and whether it is a symptom of a larger, yet undetermined sub-surface leaching problem should be developed once all surface and borehole data are assimilated and collectively interpreted.

High-resolution seismic reflection and full-wavefield seismic studies targeted key areas within and below this earthen dam. The high-resolution seismic reflection portion of the program focused on bedrock and layering within the impervious core and lower portion of pervious fill in a depth range from about 40 to 250 ft below the dam surface. Surface wave analysis provided shear wave velocity measurements in the upper 60 ft of the previous fill material that overlays the impervious dam core. These two, unique seismic measurement techniques provided key details about the materials associated with and responsible for the sinkhole.

Analysis of the shear wave velocity profiles significantly improved our understanding of the material strengths, affected shallow subsurface, and the area with the greatest risk of continued subsidence. Surface wave data from this site supports the suggestion that the sinkhole formed at the left extreme of a chimney-like structure as characterized by reduced shear wave velocities (related to stiffness) within the pervious fill. [Left and right conventions used in this report will be relative to an observer standing on the dam crest and looking downstream.] This chimney of disturbed material within the pervious fill is predominantly a left/right feature (parallel to the axis of the dam), appears quite limited in its upstream/downstream extent, and is most pronounced on profiles crossing directly through the surface depression. On profile C3 at depths greater than 40 ft below the surface of the dam the disturbed zone is approximately 40 ft wide and extends from about 5 ft left of the left edge of the sinkhole to 30 ft or so right of the sinkhole center. Located just 8 ft away, profile C4 possesses a similar reduced velocity zone more closely centered on the sinkhole and significantly less elongated to the right in comparison to C3. The 3-D geometry of this feature in the pervious fill material based on the six 2-D surface wave profiles appears to have the greatest width in the upstream/downstream direction near the surface, narrowing with depth. In contrast, the structure appears extremely elongated in the right/left "fingering" right from the center of the sinkhole as much as 30 ft.

High-resolution reflection sections provide a detailed image of the pervious fill, core, native alluvium, and bedrock surface in the depth range of about 40 ft to just over 130 ft below

the surface of the dam. Not all reflections returning from within and below the dam can be correlated to known acoustic contrasts identifiable on construction records. Reflections within the pervious fill are likely related to undocumented changes in construction materials and/or compaction practices. Cement grout and placed clay layers were unexpectedly encountered in cores from intervals where construction records indicate "native alluvium" should be present. Cement layers, unplanned placed clay layers, and variations in impervious core dimensions were likely used to remedy problems with cutoff trench stability or to improve the uniformity of the clay core. Offset in reflections at two-way traveltimes consistent with the pervious core zone is likely related to subsidence after dam completion. It is possible some subsidence occurred during construction as evidenced by the reflection droop observed in places where overlying layers appear flat. This can be seen on seismic section P1 beneath station 130 right of center of sinkhole (Figure 31). If subsidence occurred during construction, extra fill material would have been used to level the working surface to bring it back up to grade. If internal erosion is contributing to the complex geometries of reflections between 70 ms and 120 ms, significant bridging and differential compaction at the core depth will eventually migrate to the surface. During high water conditions, when hydraulic forces are the greatest, the internal degradation that is manifested in these complex reflection geometries will worsen. Distortion observed in the reflection events interpreted as defining the core wedge could be the result of stability problems during construction, subsidence after completing construction, or horizontal sampling smear.

The bedrock surface appears to have an irregular topography. Undulations on the bedrock surface are likely due to material (and therefore sediment) variability above bedrock. If the velocity function is accurate, time-to-depth conversions should compensate for these changes in material properties. However, due to the very short wavelength nature of the materials changes around the disturbed area it was not possible to fully compensate for these lateral changes in material properties using normal moveout (NMO) velocity alone. Dramatic drops in amplitude are likely related to fracture/joint zones in bedrock. It is not possible to determine if these fracture/joint systems are open or are grout sealed from construction. Subsidence below 40 ft in proximity to the sinkhole appears to be non-vertical and directionally consistent with the "fingering" interpreted on surface wave data. The core wedge appears to become more uniform upstream. Two areas with apparent fracture/joints systems and associated subsurface subsidence are interpreted with the system right of the sinkhole correlated to the sinkhole formation.

Once the drilling program is complete and crosshole seismic data interpreted, it should be possible to more definitively correlate the surface seismic data with a realistic model of the current dam interior and subgrade. Seismic techniques have rarely provided high resolution, high signal-to-noise ratio images of the interior of an earthen dam. Reflections interpretable on shot gathers are outstanding in quality and some of the best in quality and consistency we have ever recorded on the upstream slope of a dam. Irregularities in reflections on common midpoint (CMP) sections from within the pervious fill were used as indicative of disturbed areas within the dam that resulted from sediment erosion, transport, and subsidence, specifically those disturbed areas related to the sinkhole. Inversion of surface wave dispersion curves into vertical shear wave velocity profiles along a series of lines that intersected the sinkhole and ran parallel to the strike of the upstream dam surface provided low-resolution yet interpretable images highlighting areas with low/reduced compaction. Roof rock/sediment failure above voids left as a result of internal erosion, failure of dental cement within enlarged fractures in bedrock, dissolution of bedrock, or some combination of these will eventually migrate to the surface. Failure

could be instigated by increased size of void, therefore increasing roof span or increasing weight of roof rock/sediment due to excessive hydraulic head. Subsidence of layers within the dam volume appear to be directly responsible for the sinkhole.

Disturbed areas are evident on seismic reflection images in the rip-rap layer, pervious fill, impervious core, and natural alluvium from about 100 ft right and 80 ft or so left of the sinkhole. Two reasonably well defined and unique subsidence trends or areas are interpretable on reflection data below about 40 ft. Subsidence features interpreted right of the sinkhole are the most pronounced and appear to best connect with the vertical chimney structure encountered during trenching of the sinkhole and imaged on shear wave velocity cross-sections. Two smaller structures are interpreted left of the sinkhole with the larger of the two appearing to intersect bedrock near the location of an enlarged joint mapped during construction of the cutoff trench. This more extensive feature left of the sinkhole appears to have only affected the lower portion of the pervious fill material. The smaller of the two features seems either dormant or not yet large enough to have migrated vertically into the very near-surface material.

Based on data collected from borings drilled after the reflection data were collected, processed, and initially interpreted, it seems likely some irregularities observed on CMP stacked sections could be related to construction abnormalities not documented in the historical records. If the cutoff trench and core were dug and placed uniformly and the overlying pervious shell laid down in a horizontally consistent fashion, undulations in reflections from about 40 ft below ground surface down to the bedrock must have come as a result of differential settling related to either poor compaction or dissolution/erosion and subsidence. However, layers of concrete and placed clay were unexpectedly encountered in at least two of the borings. Speculation is that these materials were placed to help stabilize the cutoff trench or seal smaller joints adjacent to the two enlarged joints known to be cement filled. Borings were all placed offline and away from the areas identified as disturbed on the CMP stacked seismic sections to best accommodate the crosshole seismic study of the bedrock. The crosshole study is designed to investigate the most likely areas where interpretations of seismic reflection data indicate disturbed bedrock. As evident on the two seismic profiles separated by just over 40 ft, the material above bedrock changes quite dramatically across a very short distance within a 100 ft radius of the sinkhole.

Confirming key seismic interpretations will require drilling and sampling directly on seismic line 1 at the following locations: about 50 ft right of the sinkhole, 30 ft right of the sinkhole, and 40 ft left of the sinkhole. The six-boring pattern completed at the time of this writing was designed to surround the fractured or altered limestone bedrock area. This pattern optimizes the crosshole tomography survey but provides little or no ground truth for the surface seismic data. Enhanced confidence and improved interpretations will be possible with borings dedicated to the surface seismic reflection and surface wave data.

This study was extremely successful in optimally applying non-invasive, high-resolution seismic techniques to target internal features of an earthen dam, a goal not routinely accomplished. Reflection data from this survey possess excellent frequency content and provide high-resolution images of the pervious shell as well as impervious core. A unique, optimized acquisition geometry was used to overcome the significant physical limitations imposed on this survey as a result of working on the dam face. Layers within the pervious shell separated by distances no more than several feet were delineated and mapped. Using the tightly spaced surface wave

profiles it was possible to delineate the elongated chimney-like feature that represented the root of the sinkhole. If two or more boreholes are placed in key locations along seismic reflection line 1 it will be possible to develop an accurate map of the dam structure which should be generally consistent with the construction records, but possess significantly more detail about internal geometries than possible with construction logs alone.

Introduction

In support of the U.S. Army Corps of Engineer's strong commitment to dam safety, new and/or adaptations of existing technologies are being identified and evaluated at sites with both physical characteristics conducive to those technologies and failure potential. Proven correlation between acoustic properties and stiffness/rigidity is the basis for developing and implementing field-efficient, laterally continuous, non-invasive methods to accurately measure the seismic wavefield. As well, routine non-invasive appraisal of dam/dike core integrity is feasible and could prove quite valuable in some settings. Ultimately, the goal is to identify localized anomalous material zones—indicative of either dissolution activity or non-uniform compaction/ settling—prior to surface subsidence or the formation of vertically extensive chimney features. Seismic techniques hold vast potential for imaging and measuring materials in a fashion applicable to evaluations of dam integrity.

Clearwater Lake Dam, 30 miles northwest of Popular Bluff, Missouri, was designed and constructed in the early 1940s as a control structure across the Black River (Figure 1). During

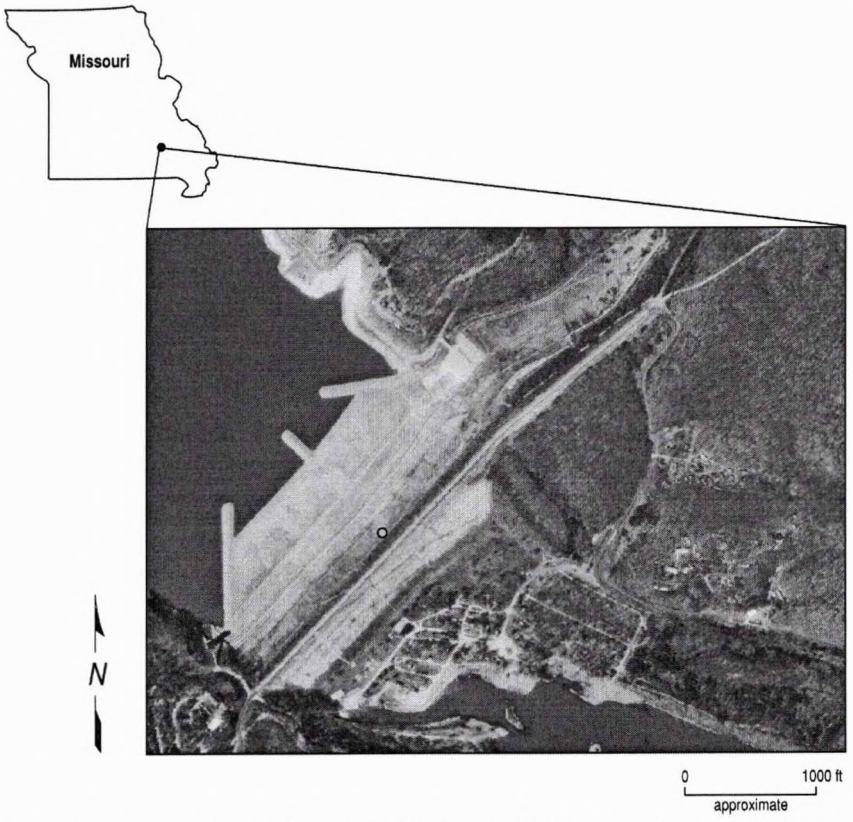

Figure 1. Aerial photo of Clearwater Dam. Sinkhole is indicated. Dikes extending into the lake were part of the 1989 retrofitting for seismic stability and seepage control.

the design and building of the cutoff trench two distinct and unique sets of enlarged joints were discovered in the limestone bedrock near stations 39+50 and 40+25 (Figure 2). Additional drilling suggested the joints were extremely localized and inferred to only extend several tens of feet beyond the cutoff trench excavation. Based on the trench and drill findings, the joints were filled with concrete consistent with the dam building practices of that time.

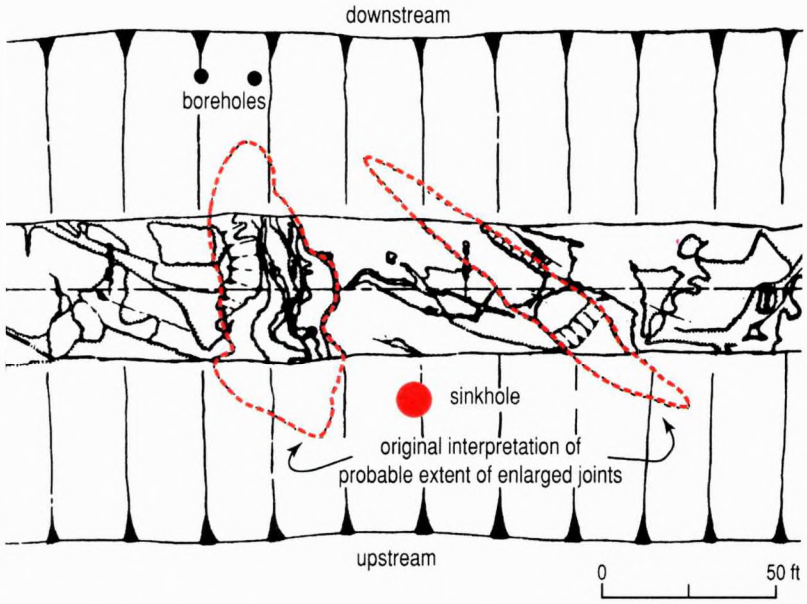

Figure 2. Joints mapped during construction of cutoff trench. Joints were filled with a custom cement mix prior to placement of engineered fill (figure provided by Hartung, 2003, USACE).

As part of a retrofit targeting seismic stability and seepage issues, clay berms were constructed in 1989 from the upstream toe of the dam out 500 ft into lake (Figure 3). Included with this retrofit was the addition of a clay blanket covering the rip-rap on the upstream slope. This clay facial formed an impervious lining on the upstream slope that extended from the upstream toe up to an elevation of 575 ft. Routine operations and pool levels were the rule through the 1990s and up until May 2002. During May 2002 a record pool of nearly 566 ft threatened to discharge through the uncontrolled spillway. During the summer of 2002 water levels were drawn down from 567 ft to 500 ft, thereby returning lake elevation to normal pool operating ranges.

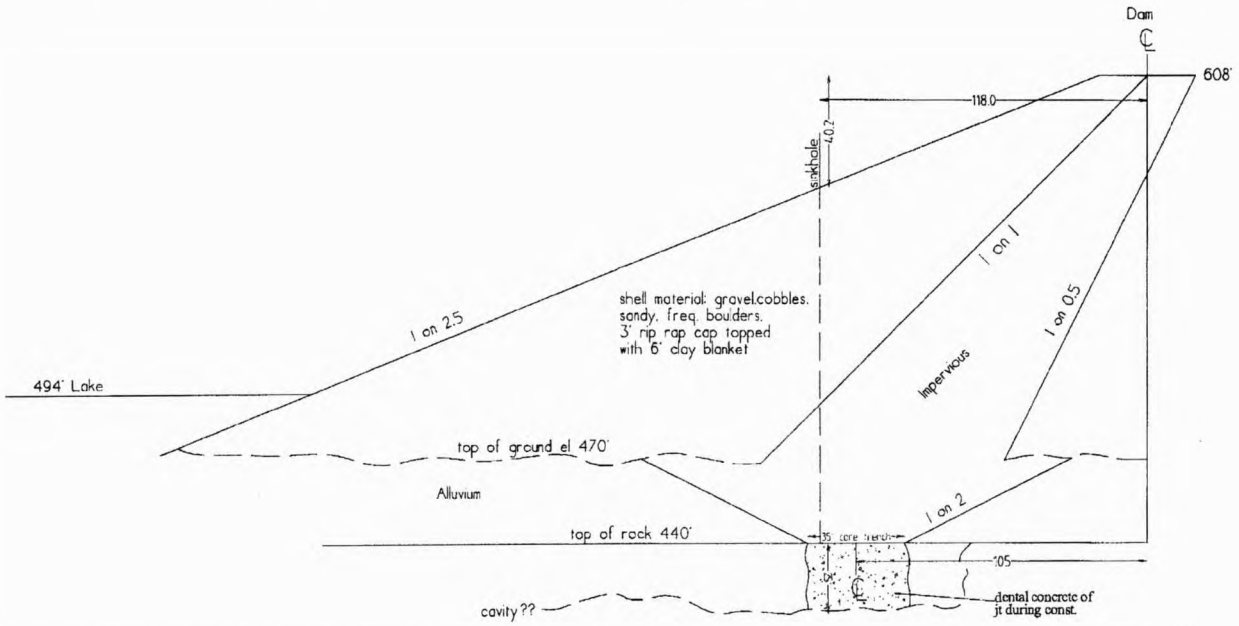

Figure 3. Cross-section of dam diagramming construction specifications and layer geometries (figure provided by Hartung, 2003, USACE).

Karst and Subsidence

In many settings around the world carbonate rocks, such as limestone and dolomite, are susceptible to solution and the formation of voids. Movement of ground water in, around, and through joints, fractures, and faults in soluble rocks can result in dissolution of those rocks and the development of cavities in the rock. A prerequisite for subsidence is the presence of voids in rocks or unconsolidated materials. Cavities formed naturally or manmade can represent a significant risk to surface activities and facilities.

Many areas in the mid-continent are underlain by carbonate rocks and can be characterized by the presence of subsurface cavities, sinkholes, and underground drainage. These anomalous rock features are called "karst terrains." Karst areas are most susceptible to sinkhole development and associated long-term subsidence. Most sinkholes form after a loss of roof rock support over voids followed by roof collapse and/or raveling. Ground water can provide buoyant support to the roofs of subsurface cavities. Lowering the water table removes this support and may result in the collapse of the roof of the subsurface cavity. Collapse of an unsupported opening or void generally results when the opening is enlarged beyond the ability of the roof rock to support or bridge the materials above. Raveling or piping is the slow erosion of unconsolidated sediments into an underground opening.

A change in the local environment that affects the soil mass can initiate collapse and subsidence. Water and its conduits to the rock are generally the most important aspects effecting change that results in subsidence. Lowering water levels is one of the most significant triggering mechanisms for subsidence in a karst terrain. Other changes that can trigger subsidence include an increase in the velocity of ground-water movement, an increase in the amplitude or frequency of water-table fluctuations, increased or induced recharge, and induced differences in hydrostatic head. Of lesser importance, but still a factor, is the increasing of roof rock load. The type and speed of change combined with the material characteristics and geologic setting control subsidence rates and volumes.

Sinkhole Chronology and Actions

On January 14, 2003, project personnel working at Clearwater Lake found a 10 ft diameter by 10 ft deep sink near elevation 573 and location 39+87 (Figure 4). A sinkhole of this nature and location represented a threat to dam integrity and prompted a response by the dam owner. On January 17, 2003, a backhoe excavated the sinkhole down to an elevation of 548 where the diameter of the subsidence feature narrowed to 3 ft (Figure 5). The 25 ft deep excavation was backfilled with a clay plug, returning the dam surface to original grade. On February 15, 2003, with the first sizeable rainfall (1.2 in) since the installation of the clay plug came subsidence of the clay plug (3 in around the perimeter and 6 in at the center). The backfilled sinkhole has been under constant surveillance since it formed with no evidence of downstream seepage, upstream slumps, cracks, or whirlpools (Figure 6). Soil engineers describe the 6 ft thick clay blanket covering the upstream slope as being very compacted and probably hiding a void that likely formed during the summer of 2002 and then finally collapsed in January, forming the sinkhole.

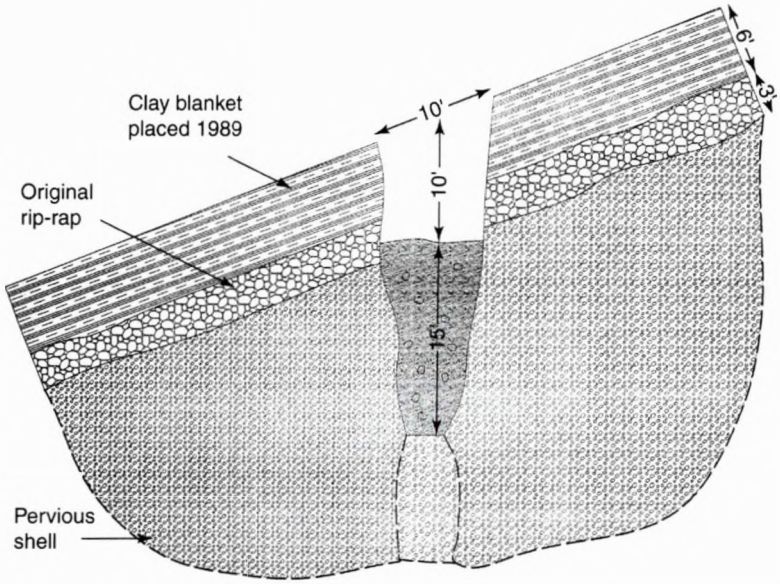

Figure 4. Material cross-section of sinkhole perpendicular to the axis of the dam. Dimensions and material classifications are based on findings of the excavation and backfill (figure from Hartung, 2003, USACE).

Figure 5. View looking northwest from crest of dam. Backhoe is process of excavating sinkhole during late January 2003 (picture courtesy of Hartung, 2003).

Figure 6. View of filled sinkhole and bench constructed to support remediation operations.

Several theories are being considered. The current "working theory" suggests the clay blanket installed in 1989 has redirected the flow of lake rises and drops in/out of the pervious shell material. Instead of lateral flow out of the dam as it was prior to placement, the clay blanket and berm cause the movement through the underlying residual alluvium and possibly through the enlarged joints discovered and grouted shut during construction of the cutoff trench (Figure 2). It seems more than a coincidence the sinkhole formed directly between and within less than 50 ft of the only major bedrock enlarged joints mapped along the approximately 2400 ft expanse of this dam. The void responsible for the sinkhole likely formed during the massive lake drawdown in the summer of 2002 but—due to the strength of the clay blanket—remained bridged until January of 2003. This "working theory" does leave several key aspects un-accounted for and therefore leaves other theories or failure mechanisms possible. For example, the spring of 2002 record pool level is one of several high pools that have been recorded since 1989 and one of several hundred high pools since 1949. Although the clay blanket may have enhanced vertical movement of water, the pathway, if it exists, has been there since construction. Another interesting observation is the eight-month delay between record high and pool subsidence. This eight-month delay in the formation of the sinkhole could be due to bridging of the clay blanket with the freeze-thaw cycle being the failure catalyst. Another possibility is a high seepage gradient accelerated during high pool in the spring of 2002 migrating to the surface through subsidence over decades. The presence of the sinkhole over one of the only two crevasses to pass fully beneath the core trench might be more than just a coincidence associated with construction defects.

Program Objectives

Geophysics used during site characterization routinely involves relatively noisy measurements of earth properties, qualitatively incorporated into working subsurface models with ground truth provided by observational data sets (e.g., drilling, outcrop studies, etc.). Evaluation of dam and dike integrity and internal structures complicates and usually eliminates effective use of many geophysical tools due to layer geometries, conductive materials used during construction, utilities and operational workings, depth of investigations, and resolution requirements. Body wave seismic techniques have not been extensively used due to survey costs and resolution requirements. With equipment improvements, technique developments, and the wealth of information contained in the seismic wavefield (body waves and surface waves), seismic measurement or imaging data are routinely underutilized (Steeples et al., 1995).

This applied research project was designed to evaluate the applicability of several seismic techniques to identify, evaluate, and delineate key physical characteristics and/or material properties associated with failure risk within and beneath Clearwater Dam. High-resolution seismic reflection has been reasonably successful imaging unconsolidated materials from about 30 ft below ground surface to depths in excess of several hundred feet. As well, detection of fractures in sedimentary rocks has been a routine objective of seismic reflection surveys. Multichannel surface wave inversion techniques (MASW) have proven capable of detecting anomalous shear wave velocity zones within and below fill materials (Miller et al., 1999). Shear wave velocity studies of fill materials provide a general understanding of key engineering properties like stiffness and Poisson's ratio, leading to an increased awareness of areas susceptible to ground failure.

Program Components

Reflection

Seismic reflection is a sound imaging tool that relies on velocity/density contrasts in the subsurface that will reflect sound waves produced and recorded on the ground surface (Appendix A). A properly designed and executed high-resolution P-wave seismic reflection survey should be capable of mapping the bedrock surface and discriminating variations in seismic attributes indicative of major changes in the integrity of bedrock. Key to the effectiveness of this tool at Clearwater Dam was the generation of high resolution (>120 Hz P-wave) reflection signals and low frequency, broadband surface wave energy; optimizing 2½-D spread design; tailoring processing flows to optimize the accuracy and spatial distribution of subsurface sample points; and integrating interpretations of P-wave reflections with the S-wavefield, dam construction information, and drill data. Proven high-resolution concepts were used to guide the design of data acquisition parameters and selection of the optimum equipment and methodologies for this site and objectives (Steeples and Miller, 1990).

For the reflection data to be useful in delineating bedrock fractures it is imperative to maximize the resolution potential, interpretability, and signal-to-noise ratio of reflection returning from within the dam. Intra-dam reflections provide improved time-to-depth conversions and a relative guide for determining real structures and anomalies observed on reflections from bedrock from artifacts. To maximize the chance of recording reflections from within the dam

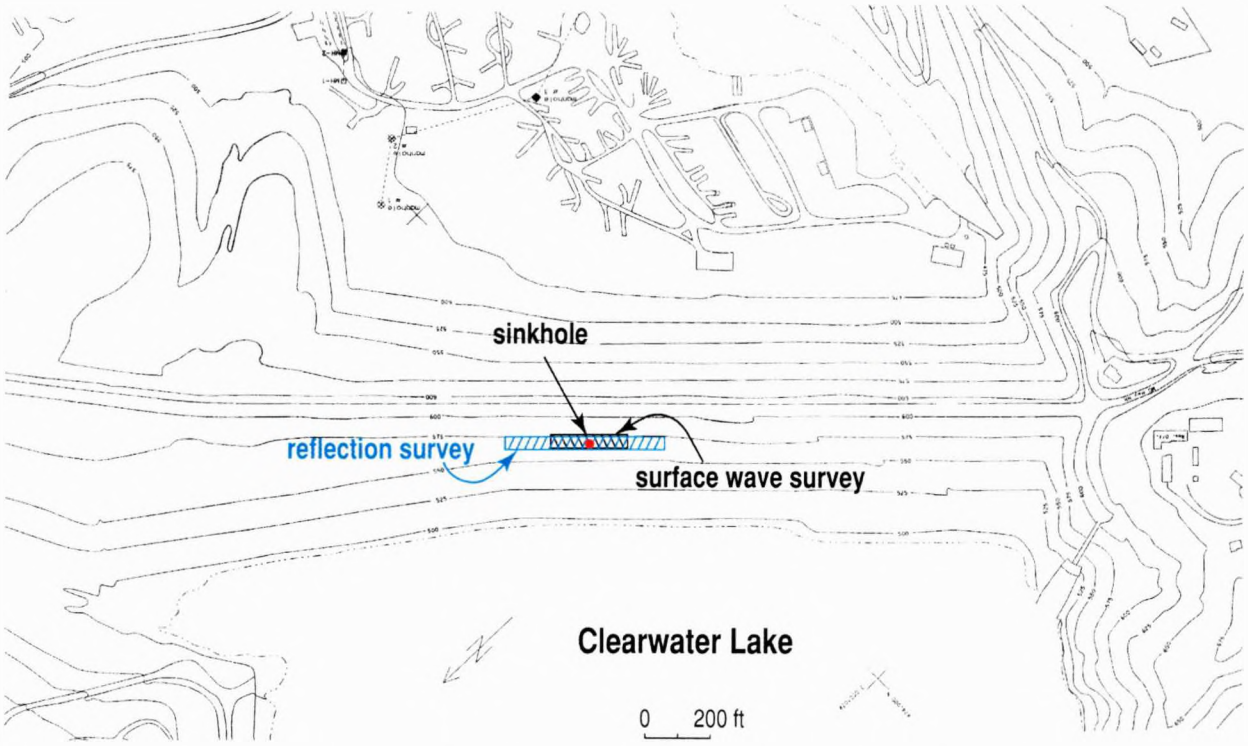

Figure 7. Site map with elevation contours, sinkhole, and planned locations of two seismic profiles (surface wave/ tomography and high-resolution reflection).

and alluvium beneath the dam, two CMP profiles (Mayne, 1962) were acquired using a single source line (located just above the sinkhole, along the access road at the top of the clay blanket) and two parallel 120-channel fixed spreads (one through the sinkhole and one below the terrace built around the sinkhole) offset from the source by 10 ft and 45 ft (Figure 7). This geometry was designed to maintain the optimum recording window and image the subsurface parallel to the dam axis, straddling the sinkhole's subsurface expression (Hunter et al., 1984). Data were acquired and processed to delineate local irregularities in stratigraphy, structure, and material properties from about 40 ft below ground surface to as deep as 250 ft below ground surface.

Data acquisition and processing for the 2-D profile data generally followed well-established shallow high-resolution data acquisition methodologies, emphasizing correlation with ground truth, shear wave velocity profiles, and optimized velocity control for reflection coherency and resolution and accuracy of time-to-depth conversions (Hunter et al., 1984; Knapp and Steeples, 1986; Steeples and Miller, 1990).

Surface Wave Inversion

Surface waves traditionally have been viewed as noise in multichannel seismic data collected to image targets for shallow engineering, environmental, and ground water purposes (Steeples and Miller, 1990). Recent advances in the use of surface waves for near-surface imaging have combined spectral analysis techniques (SASW)—developed for civil engineering applications (Nazarian et al., 1983)—with multi-trace reflection technologies—developed for near-surface (Schepers, 1975) and single-spread multichannel petroleum applications (Glover,

1959). The combination of these two unique approaches to seismic imaging of the shallow subsurface permits non-invasive estimation of shear wave velocities and delineation of horizontal and vertical variations in near-surface material properties based on changes in these velocities (MASW) (Park et al., 1996; Xia et al., 1999; Park et al., 1999).

Extending this imaging technology to include lateral variations in lithology as well as void and fracture detection, bedrock mapping, and subsidence/karst delineation has required a unique approach that incorporates SASW, MASW, and CMP methods. By integrating these techniques, 2-D continuous shear wave velocity profiles of the subsurface can be generated. Estimating the dispersion curve from up to 60 closely spaced receiving channels calculated every 4 to 8 ft along the ground surface enhances the signal and results in a unique, relatively continuous view of shallow subsurface shear wave velocity properties. This highly redundant surface wave method improves the accuracy of calculated shear wave velocities and minimizes the likelihood that irregularities resulting from erratic dispersion curves will corrupt the analysis.

Surface wave data were acquired on six lines crossing the sinkhole parallel to the dam axis (Figure 7). Data were acquired simultaneously on two adjacent 120-station lines with the energy source moving incrementally from shot station to shot station between the two recording lines. Each profile used the same spread geometry and numbering sequence relative to a line perpendicular to the dam axis that split the sinkhole in half. Acquiring these data in this fashion permitted excellent line-to-line correlation and made it possible for 2½-D interpretations of the shear wave velocity field. With the unique requirements of surface wave measurements it was imperative to use an accelerated weight drop source, low-frequency receivers, and close receiver spacing.

Data Acquisition

Experimental (Testing) Phase

Experiments mainly consisted of walkaway noise tests, which are single fixed-spread deployments designed to allow evaluation of a variety of source configurations. All data for this study were recorded on a 24-bit, 240-channel Geometrics StrataView seismograph with a StrataVisor NZC controller. The testing included energy recorded from source-to-receiver offsets ranging from 8 ft to approximately 400 ft (Figure 8). The receiver intervals used during testing were 2 ft for the 4.5 Hz Geospace GS11D and 4 ft for the Mark Products L28E 40 Hz recievers. The Rubberband Assisted Weight Drop (RAWD) and IVI Minivib high frequency vibrator were the sources selected for surface-wave and P-wave data acquisition (respectively) based on their mobility, near-surface conditions, target depth, recorded frequency bandwidth and dominant frequency, and environmental constraints (Figures 9a and 9b). The minivib, a non-invasive high-frequency vibrator, will produce 3 psi ground pressure for minimum ground deformation and optimum mobility while providing over 4000 lbs of force at 200 Hz. The RAWD, on the other hand is a small, maneuverable, impulsive, non-invasive weight drop that delivers a seismic pulse with a significant low-frequency component to the wavefield. Equipment and parameters tested were selected based on site conditions, project objectives, and experience.

Figure 8. View of test lines, one across the sinkhole and one downstream of the sinkhole. Wood stake marks downstream edge of sinkhole.

Figure 9a. Rubberband Assisted Weight Drop (RAWD) mounted on a tracked Case skid-steer loader working along the upstream dam face.

Figure 9b. IVI minivib high frequency vibrator.

Production Acquisition

Data were acquired using different spread geometries for the two different types of data. All source and receiver lines were generally centered on the sinkhole (Figure 7). Energy recorded by two sub-parallel receiver lines was from a single energy source moving along an offset source line (Figure 10). This orientation provided twice the number of subsurface sample points per shotpoint, thereby improving the economics and the spatial sampling interval of the resulting sections. Two receiver lines and one source line were used for the reflection data and six receiver lines and three source lines provided the best subsurface coverage for surface wave data, considering the site limitations (Figure 11).

For ease in working on the sinkhole with heavy equipment a clay bench was constructed to provide a level working surface on the side of the dam (Figure 12). This clay bench complicated the data processing partly due to the nearly 3 ft change in elevation for receivers placed on the bench versus those into the clay blanket (Figure 13).

Unique geometries and equipment were necessary to optimize these two techniques for different portions of the subsurface, physical earth properties, and resolution requirements. For the reflection data, a pair of 120-channel lines with two 40 Hz L28E geophones per receiver station recorded three 10 second, 25 to 250 Hz IVI minivib sweeps at each shot station (Figure 14). All reflection ground stations were separated by 4 ft. Surface wave data are four-shot vertical stacks of RAWD impacts that were recorded by two 120-station receiver lines each with a single GS11D 4.5 Hz geophone at each receiver station (Figure 15). Source and receiver stations for surface wave data were separated by 2 ft. Surface wave lines were about 240 ft long and extended about 50 ft upstream from the edge of the road at the top of the clay blanket. Reflection lines were almost 500 ft long with the most upstream line about 50 ft from the upstream edge of the road at the top of the clay blanket. These acquisition parameters provided dense subsurface coverage over the area that appeared from surface investigations and construction documentation to be the most likely volume responsible for the sinkhole (Figure 11).

Several reflecting events are easily interpretable at times between 40 and 120 ms (Figure 16). Considering the velocity and near-surface conditions of this earthen dam structure, these reflections are of outstanding quality and quantity. With dominant frequencies around 200 Hz, NMO of 1500 ft/sec to 2500 ft/sec, and reflection hyperbolae that extend completely through the noise cone, resolution and signal-to-noise are much higher than expected. Using a practical vertical resolution limit of ½-wavelength and the radius of the Fresnel Zone as the fully resolvable horizontal limit, beds as thin as 4 ft and objects as small as 30 to 40 ft in diameter can be resolved.

Fundamental surface wave energy possesses excellent dispersive characteristics with a frequency range from 35 Hz down to as low as about 3 Hz, providing excellent penetration and near-surface resolution. Shot records of surface wave energy (Figure 17) differ markedly in appearance and wave properties in comparison to reflection shot gathers (Figure 16). The dominant energy traveling across the record is the surface wave, also known as ground roll. With the excellent dispersive characteristics and frequency content evident in the shot gather it is no surprise that the dispersion curve is well formed and can be concisely interpreted (Figure 18).

Figure 10. (above) View of RAWD traveling between two surface wave profiles (C1 and C2).

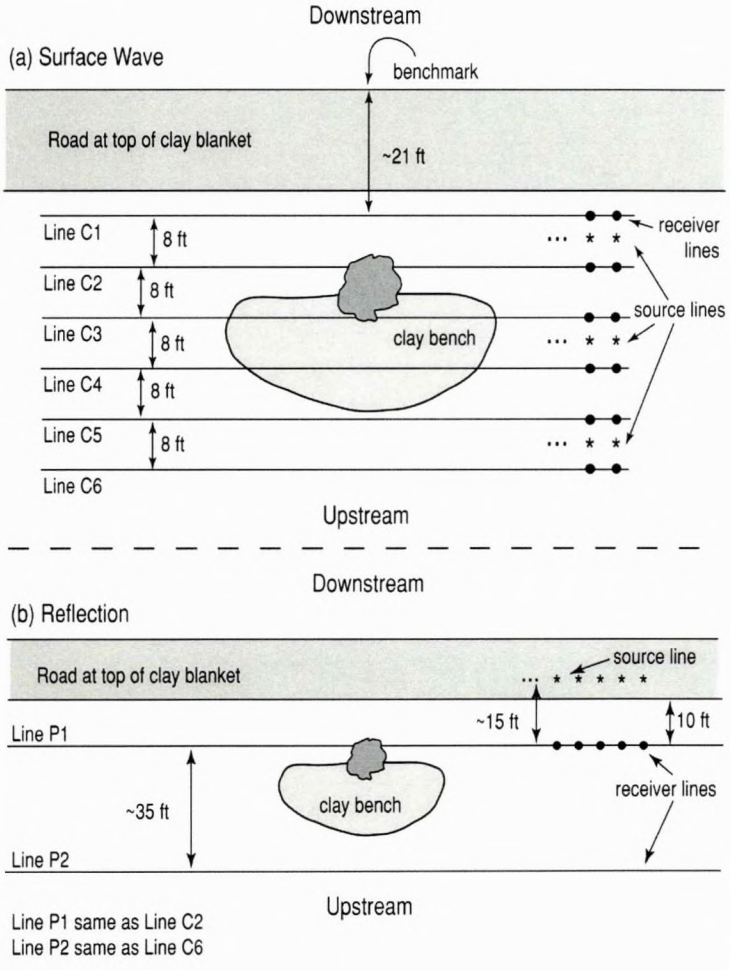

Figure 11. (left) Line layout for surface wave data (a) and reflection data (b).

Figure 12. View of vibrator working above sinkhole. The clay bench built to allow sinkhole remediation is evident.

Figure 13. View of back side of clay bench clearly showing the 2 to 3 ft high terrace.

Figure 14. View of vibrator and seismograph (John Deere Gator with yellow cover) deployed along reflection lines.

Figure 15. RAWD and seismograph (John Deere Gator with yellow cover) deployed along surface wave lines.

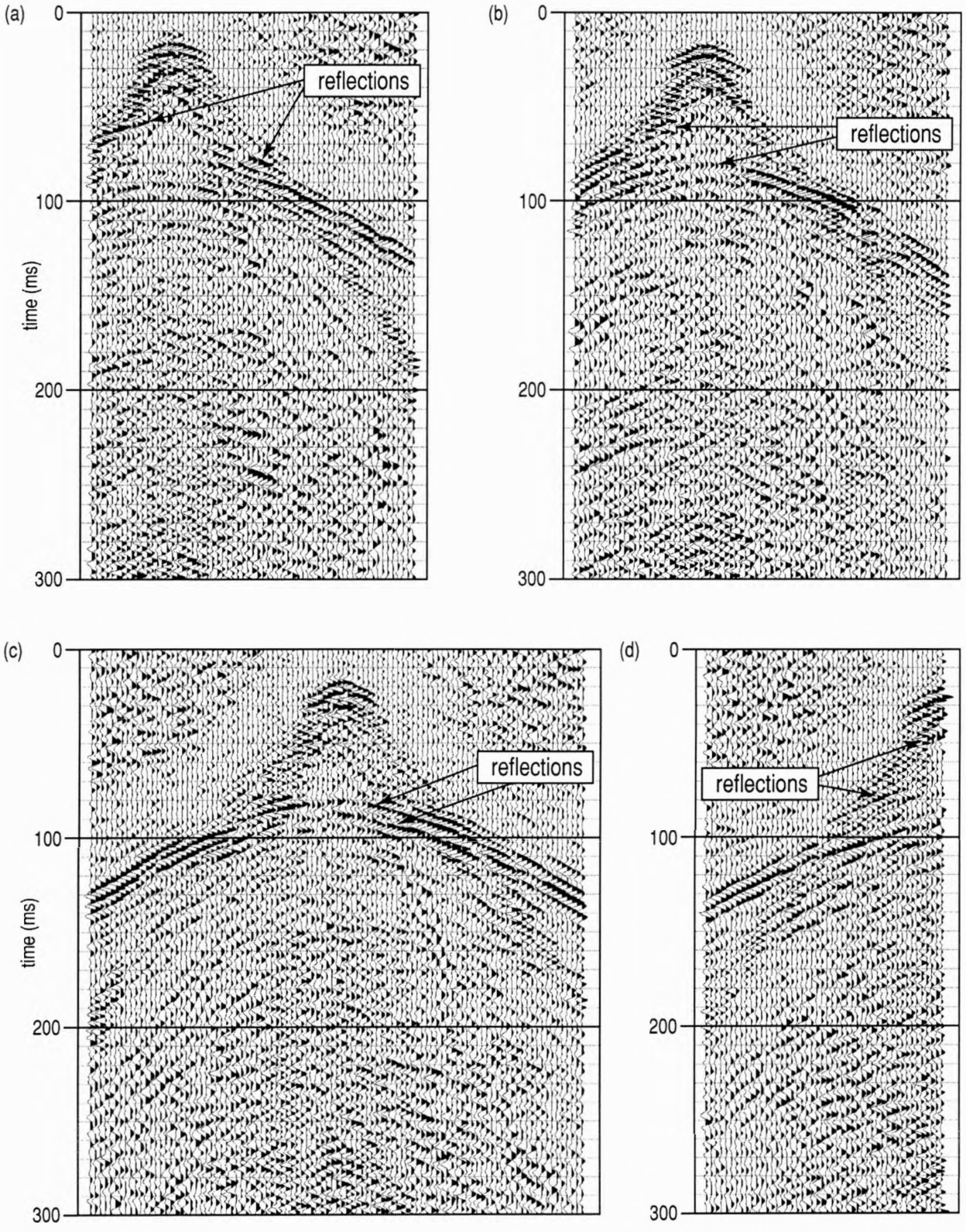

Figure 16. Representative shot gathers from across line P1. Reflections are evident on all these spectral balanced shot gathers. Based on stacking velocities, reflections from 80 ms are approximately 100 ft deep.

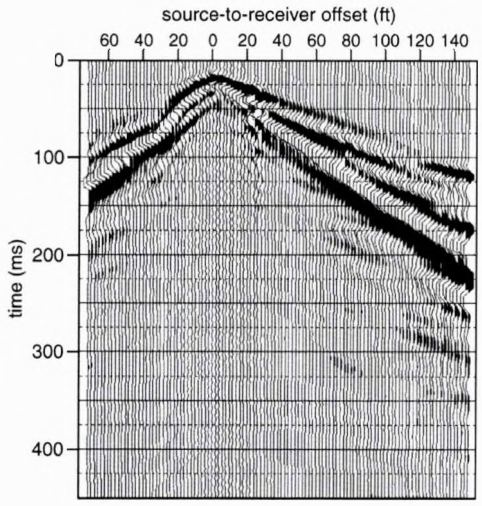

Figure 17. Surface wave shot gather.

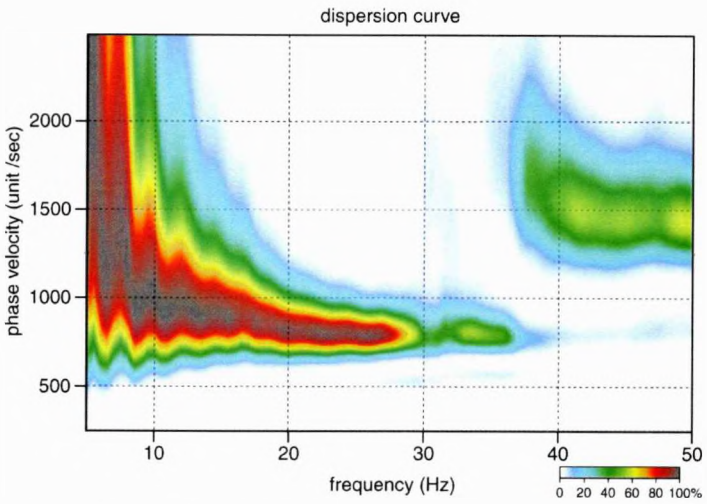

Figure 18. Surface wave dispersion curve.

Penetration depths based on the half-wavelength estimates could reach 50 to 60 ft, providing reliable shear wave velocities to those depths.

Data points were surveyed in using a differential GPS unit sold by Trimble (Figure 19). The system included a 4700 base and 4800 rover unit, providing x, y, and z accuracy of less than 1 inch. Line placement was dictated by location of the sinkhole, steepness of the upstream dam face, geometry of the sinkhole, and construction information. GPS readings were taken at key benchmarks and as many of the receiver and source stations as possible.

QA/QC

Data acquired and processed on this survey were managed to ensure the highest quality and most accurate acoustic representation of the subsurface possible. State-of-the-art techniques were used in a fashion that is appropriate and verified with step-by-step QA/QC. The most important (possibly even essential) information monitored during acquisition and processing were shot gathers (Figures 16 and 17) and dispersion curves (Figure 18). This information allows

Figure 19. GPS coordinates were measured by a Trimble system including a 4700 base and 4800 rover unit.

the geophysicist and geologist to make determinations as to the authenticity of processed seismic sections. Seismic processing software and techniques are very powerful tools that, if not used properly, may result in unrealistic interpretations.

The equipment and recorded data were continuously monitored during acquisition to ensure the highest quality sections. Receiver response was evaluated using relative amplitude comparisons for side-by-side modified tap tests performed after the planting of each geophone or group of geophones. The continuity and leakage of each active station was electronically measured with a 20% range of acceptable coil impedance centered on the factory specifications and leakage not exceeding 5M ohms. Visual analysis of the general signal-to-noise ratio, phase velocity and consistency of environmental noise, DC bias, and variations in the optimum recording window was performed on at least every fifth field plot.

Data Processing

Seismic Reflection

High-resolution seismic reflection data, by its very nature, lends itself to over-processing, inappropriate processing, and minimal involvement processing. Interpretations of high-resolution shallow reflection data must take into consideration not only the geologic information available, but also each step of the processing flow and the presence of reflection events on raw unprocessed data. Processing for the reflection portion of this study included only operations or processes that enhanced signal-to-noise-ratio and/or resolution as determined by evaluation of high confidence reflections interpreted directly on shot gathers (Figure 20). For the most part, processing of high-resolution shallow reflection data is a matter of scaling down conventional processing techniques and methods; however, without extreme attention to details, conventional processing approaches will produce undesirable artifacts. In-field processing of the reflection data resulted in correlated shot gathers that were subject to a variety of scaling and filtering operations. In-field processing was coincident with data acquisition and did not impact the full day field schedules.

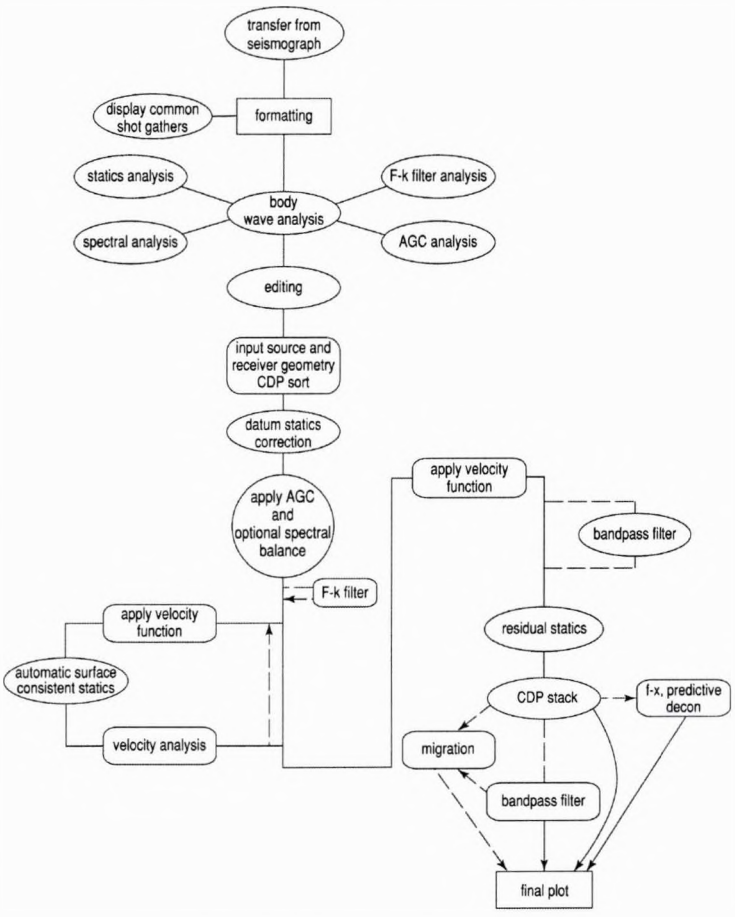

Figure 20. Generalized processing flow.

The basic architecture and sequence of processing steps followed during the generation of the final stacked sections were similar to conventional petroleum exploration flows (Yilmaz, 1987). The primary exceptions related to the step-by-step QC necessary for the highest confidence interpretations of shallow features and realization of full resolution potential (Miller et al., 1989; Miller et al., 1990; Miller and Steeples, 1991) (Figure 20). Specific distinctions relate to the emphasis placed on velocity analysis (Miller, 1992), lack of extensive wavelet processing, care and precision placed on muting, step-by-step analysis of effects of each operation on reflected energy, limiting statics operations to maximum shifts no greater than one-quarter wavelength of the dominant reflection energy with large correlation windows, and coincident iterative velocity and statics analysis.

Convert to KGS
Bulk static 400
AGC scale 1000
Cross-correlate w/synthetic (30 Hz-400 Hz) (taper 1s-0.25s)
Analyze shot gathers
F-k filter tests
spectral balance (30-40—300-400)
Edit
    Mute air coupled wave
    Remove First arrival
    Kill bad/dead traces
Apply geometry
Offset limiting edit
Vertical stack w/consistent shot station
Secondary edit, remove noisy traces
Sort CMP
Velocity analysis (1250 ft/s to 3000 ft/s)
NMO correction 0.75 stretch mute
VELF 2018 45 1500 86.5 1750 106 2000
VELF 2068 37 1750 77 2000 120 2250 127.5 2500
VELF 2118 50 1500 70 1750 131 2250
VELF 2168 45 1750 82 2000 129.5 2500
VELF 2218 81.5 1750 100 2000 139.5 2500
Residual static 4 ms max shift 80 ms correlation window
CMP stack
AGC scale (100 msec)
Migration (velocity [m or ft/s]: 2000; trace spacing 4 ft)

Figure 21. Reflection processing flow for Clearwater data.

Each analysis step in the processing flow and key parameters defined for each operation allows a reasonable critique of the CMP stacked sections (Figure 21). Any additional information about the processing flow or parameters can be provided within a reasonable amount of time (amount of time determined jointly). Any digital information can be delivered upon request in the native format of each (data is either SEG2 or KGS, graphics are .pcx or .jpg). All hardcopy displays of requested data will be provided as 300 dpi plots. Horizontal and vertical scale on hardcopy displays will be set to maximize the analysis potential of these and existing data.

Surface Wave

To ensure accurate and consistent MASW results it is imperative to process only the optimum traces (selection based on source-to-receiver distance for a particular target interval) from each shot gather. For these data about 30 traces per gather were analyzed using the software package SurfSeis (a proprietary software package from the Kansas Geological Survey that facilitates use of MASW for continuous profiling). Each shot gather (Figure 17) was transformed to produce one dispersion curve and assigned a surface location corresponding to the middle point of the spread (Figure 18). Care was taken to ensure that the spectral properties of the t-x data (shot gathers) were consistent with the maximum and minimum f-v_c values (v_c is the phase velocity of surface waves) contained in the dispersion curve. Estimating the dispersion curve in this fashion is both robust and allows identification and removal of coherent source noise on both the shot gather and dispersion curve (Park et al., 1998). Inverting the dispersion curve produces

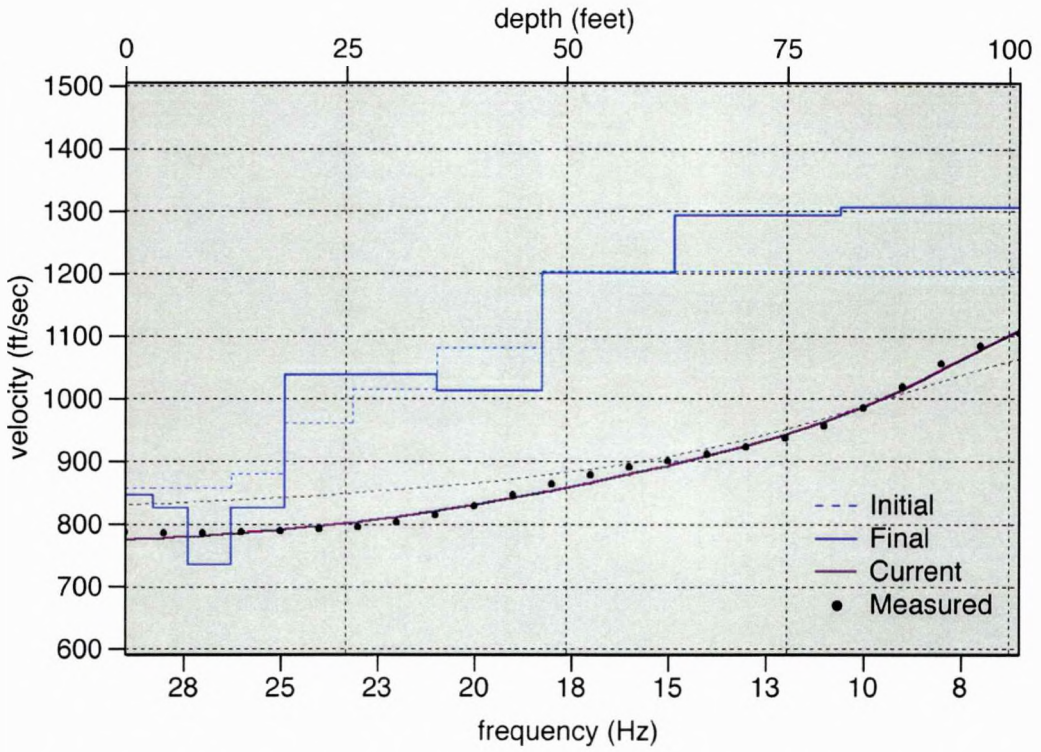

Figure 22. Shear wave velocity profile determined by inverting surface wave dispersion curves.

a shear-wave velocity profile as a function of depth (Figure 22). Assumptions necessary for this inversion, such as Poisson's ratio, density, and layer model, can be made with confidence considering the dependence of each on the shear wave velocity profile (Xia et al., 2000). Each shot gather produces a single velocity-with-depth trace that, when combined with velocity traces from all the shots along the survey line, produced 2-D shear wave velocity maps.

Interpretation

Surface Wave

Interpretations for this report are limited to identifying changes in subsurface layer geometry; amplitude, frequency, and phase characteristics that appear to relate to subsurface non-uniformities; and lateral variations in seismic properties. Shear wave velocity is commonly used as a measure of material rigidity or stiffness. Lateral changes in material properties are most obvious on 2-D shear wave images produced using continuous profiling techniques. Interpretation of shear wave velocity profiles for this investigation mainly focused on drops in shear wave velocity that could be correlated to the sinkhole location. Considering the age and construction of this earthen dam, compaction is going to naturally vary independent of any current or previous dissolution/erosion related activities. Changes in compaction could manifest themselves in reflection droop or shear wave velocity changes unrelated to the subsidence responsible for the sinkhole formation.

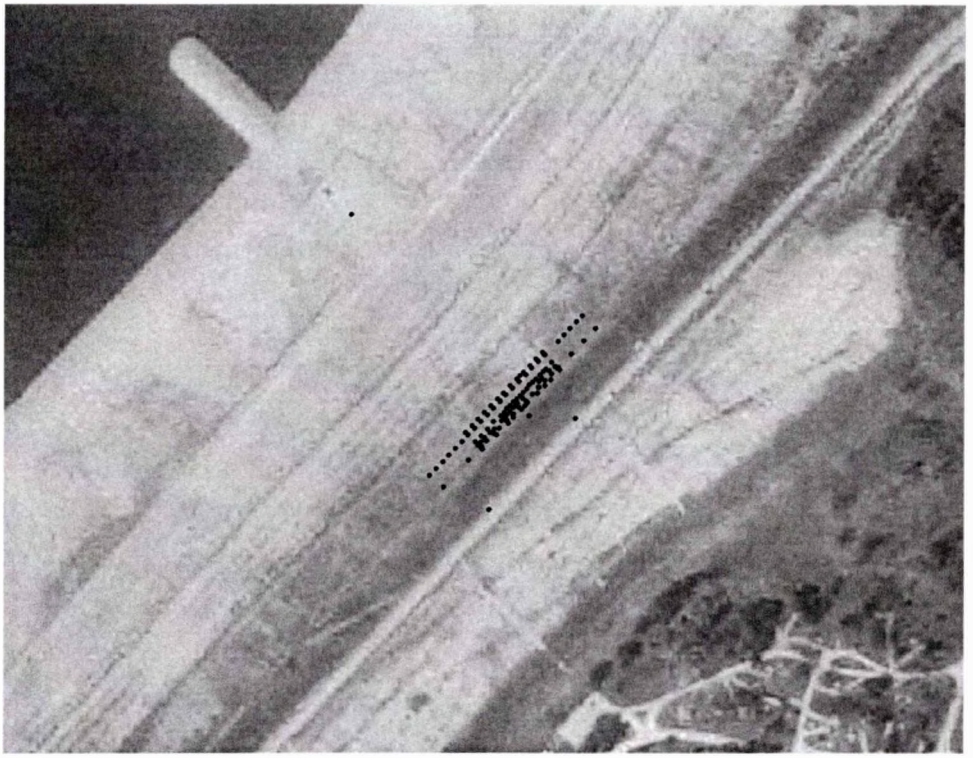

Figure 23. Various receiver stations superimposed on an orthophoto of Clearwater Dam.

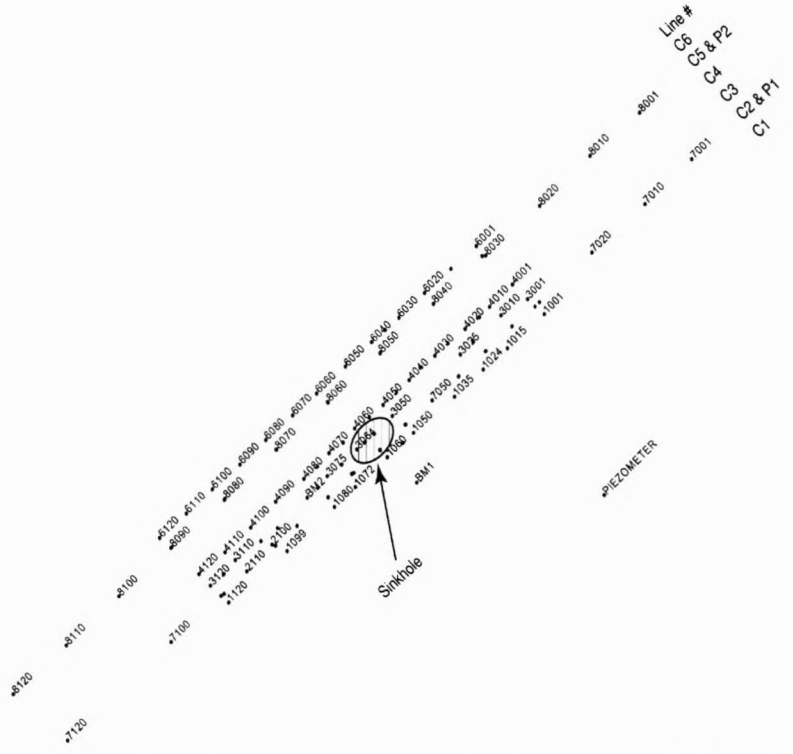

Figure 24. Various receiver points identified by station number and line in relation to the sinkhole on the dam.

Figure 25. View of flags marking stations for reflection survey.

Shear wave velocity profiles targeted the upper 40 ft or so of the dam, focusing predominantly on areas near and below the sinkhole currently exhibiting characteristics consistent with zones of potential structural weakness. Data on some lines possessed sufficient low frequencies to allow interpretations of features as deep as 80 to 90 ft. The upstream extent of the subsurface disturbed zone associated with the sinkhole was of the greatest interest. One surface wave line was recorded downstream of the sinkhole, two over the sinkhole, and three were recorded upstream of the sinkhole. There appears to be little or no abnormality in the shear wave velocity downstream of the sinkhole. Only the first profile upstream (C4) seems to have a subsurface signature consistent with predicted subsidence effects on shear-wave velocity. Clearly from the surface wave data, the "root" of the sinkhole is a chimney-type structure and evident on profiles that cross directly through the sinkhole and one immediately upstream of the sinkhole.

Line C2 passes across the downstream edge of the sinkhole and might have a very subtle change in shear wave velocity that could be interpreted as subsidence related (Figure 26). Clearly below about 20 ft there is no evidence of weak zones beneath line C2. The most noteworthy feature along this line is the high velocity feature about 40 ft left of the sinkhole center. This high velocity feature is very vertical and seems to extend from the dam surface completely through the 50+ ft deep imaged zone. Another similar but much more subdued high velocity feature can be seen 60 ft right of the sinkhole center. The high velocity zone 40 ft left of the sinkhole strongly influences all the intermediate layers as is most evident in the green velocity zone at around 30 ft below ground surface

Line C3 provides the most dramatic view of the sinkhole "root" (Figure 27). From the line C3 cross-section it appears that the affected subsurface is around 40 ft wide predominantly in the right/left directions. Near-surface (upper 20 ft) the subsurface footprint of the sinkhole is

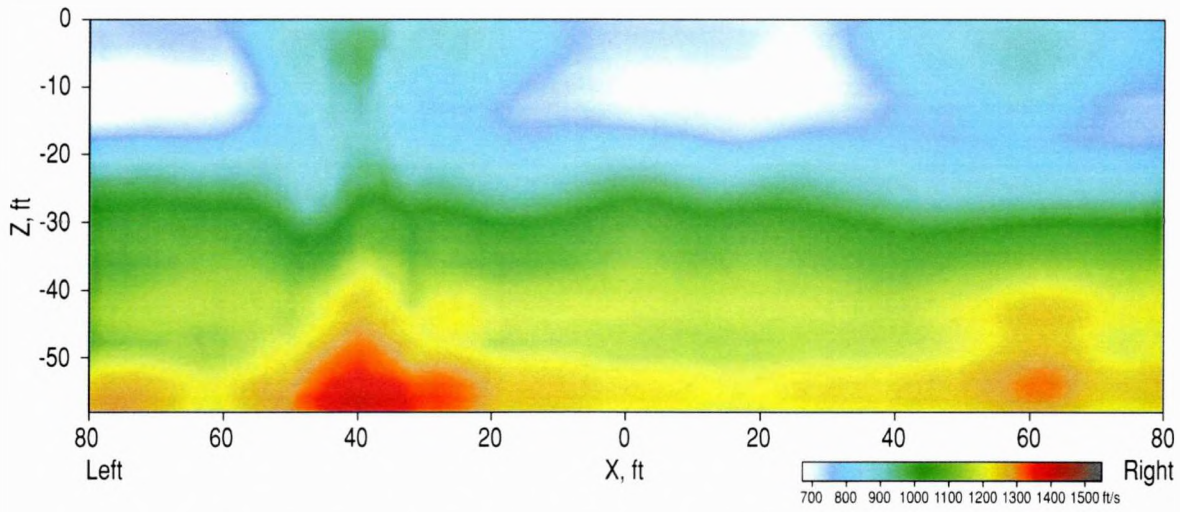

Figure 26. Clearwater Dam, Line C2, Vs, ft/s, 9-17 Hz frequency range.

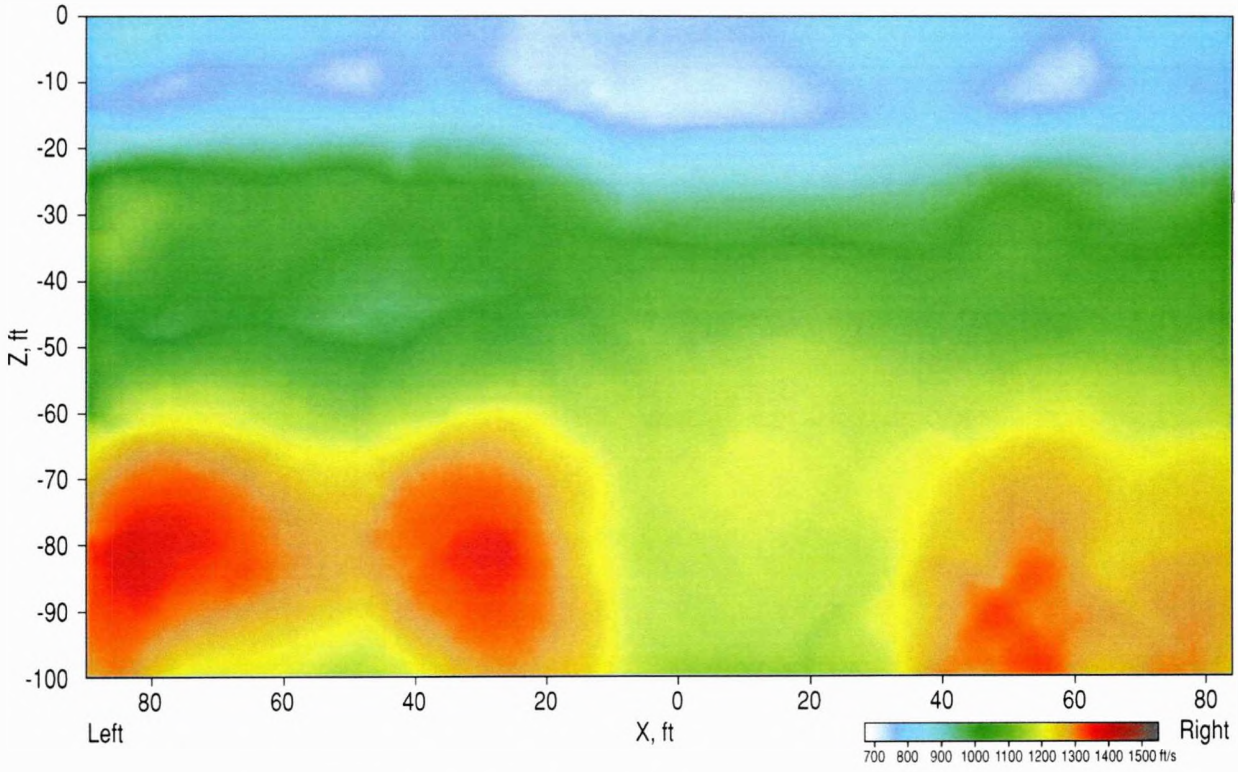

Figure 27. Clearwater Dam, Line C3, Vs, ft/s, 6-28 Hz frequency range.

well constrained and appears to be about 10 ft wide with some minor velocity reductions extending as far as 20 ft from the sinkhole center to the right. This wide zone of influence is not unexpected or inconsistent with the trenching that was completed near the time the sinkhole was discovered. Vertical trenching suggested the subsidence was 10 ft wide at the ground surface narrowing to a diameter of just a few feet at around 20 ft below ground surface. This disturbed cone has a zone outside the physical subsidence area that will have altered shear wave velocities much larger than the subsidence feature itself. Clearly below 30 ft the zone of marked influence increases to almost 40 ft, asymmetric to the right of the sinkhole itself.

Mapping just the lowest velocity material and therefore looking at the largest lateral shear wave velocity gradient on line C4, the 10 ft diameter sinkhole appears well defined and very vertical (Figure 28). Shear velocity gradient is represented as lateral changes that extend over several stations. However, at increasing depths below 20 ft the footprint of the sinkhole becomes more pronounced with a more complex failure pattern below 60 ft than the simple sagging layers apparent above about 20 ft. Without line C3 (Figure 27) it would be difficult to accurately place the subsurface area associated with the sinkhole on line C4 (Figure 28). Some of the variability in shear velocity is clearly related to non-uniform construction practices (e.g., drop in shear velocity at 25 ft below station 40 ft to 20 ft left of the center of the sinkhole). A localized drop in shear velocity below 60 ft is interpreted as related to the sinkhole. It is likely the subsurface expression of the sinkhole becomes irregular at these depths and in this case begins to enlarge upstream, but to a much smaller degree than it extends right at these same depths as evidenced on line C3.

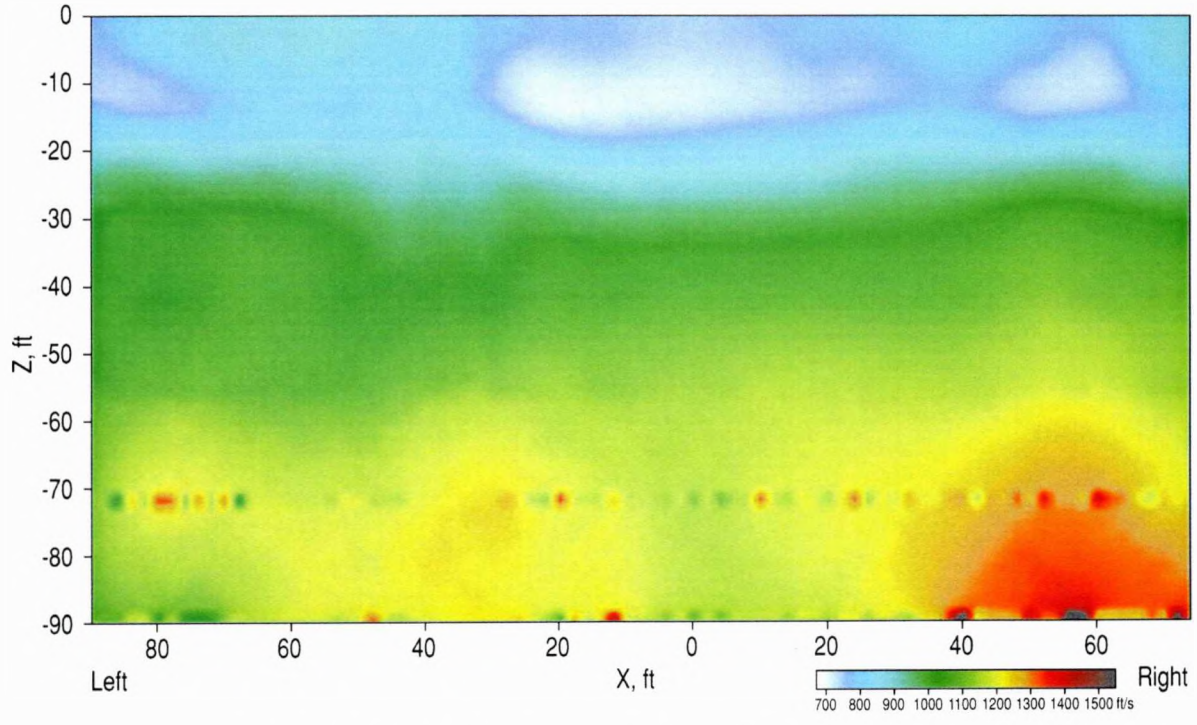

Figure 28. Clearwater Dam, Line C4, Vs, ft/s, 6-28 Hz frequency range.

Shear wave velocity profiles from lines C5 (Figure 29) and C6 (Figure 30) do not appear to have sampled the same characteristic low shear wave velocity zone interpreted here to be associated with the sinkhole and subsurface subsidence. The relatively uniformly layered media with a gradually increasing velocity function would be expected for the native undisturbed dam materials. Some undulations in the velocity function left of the sinkhole around 20 ft and 60 ft are not large enough to be a concern, and are likely related to construction variability. Interpreting such subtle features on surface wave data alone must be done with extreme caution, only suggesting the many possible reasons for such a feature.

Looking collectively at the six surface wave lines a few features are noteworthy and likely significant to this investigation. First, the altered subsurface associated with the sinkhole appears slightly upstream of the sinkhole center and elongated to the right. Upstream the root of the sinkhole is enlarged at depth, but does not extend as far as lines C5 or C6, therefore it is less than 30 ft long in upstream/downstream direction at around 60 ft below ground surface. It does, however, extend around 40 ft right of sinkhole center along line C3, which skirts the upstream edge of the sinkhole. The remaining lines (with a sinkhole expression—C2 and C4) only showed reduced shear wave velocity interpreted as related to the sinkhole in a right/left direction around 10 to 20 ft.

Second, a very noticeable high velocity chimney feature is visible on lines C2, C3, and C4 around 40+ ft right of the sinkhole center. Also, noteworthy is the high velocity feature on both C2 and C3 between 20 ft and 40 ft left (Figures 26 and 27). These high velocity features are not consistent with the velocity characteristics of areas with reduced strength usually associated with failed sediments. Of possible significance is the effect on shear wave velocity when the stress/strain relationship as defined by Young's Modulus becomes non-linear with extreme strain. In that situation the shear wave velocity increases as stress builds beyond the relationship of stress and strain as defined by Young's Modulus. This scenario has been observed pre-failure in mines where roof rock spans exceed rock strength. It has also been observed in karst areas prior to the formation of a sinkhole. This is not to say a sinkhole will form that correlates with these higher velocity zone; these high velocity zones have been shown to correlate to high stress zones in rock, not unconsolidated materials. Localized increases in shear velocity are usually associated with rock approaching failure levels. No empirical observations have been published of increased shear velocity associated with pre-failure in unconsolidated or even over-compacted sediments.

Seismic Reflection

Common midpoint (CMP) stacked sections provide an excellent glimpse into the internal layer geometry from bedrock to about 40 ft below ground surface. Taking data from shot gather format to CMP stacked sections includes a loosely defined set of steps that result in a seismic cross-section with time translating to depth by the average sediment velocities (Appendix A). To ensure the safety of the operation, the IVI minivib was used only along the road at the top of the clay blanket and therefore reflection data were acquired using a single source line (along the access road at the top of the clay blanket) and two parallel lines offset from the source 15 ft and 50 ft and straddling the sinkhole (Figure 11). Reflection frequencies were quite high considering the nature of the man made fill that composes this dam. Interpretable reflections are evident from about 50 ms to more than 100 ms on line P1, translating to a depth range from around 30 ft

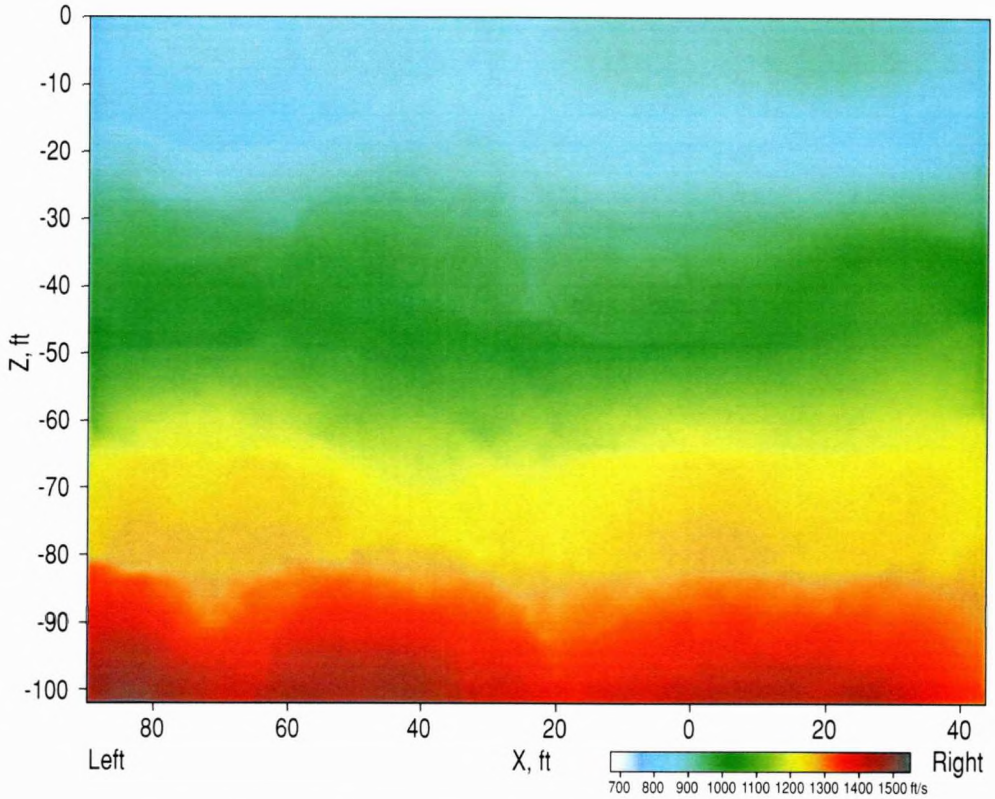

Figure 29. Clearwater Dam, Line C5, Vs, ft/s, 6-28 Hz frequency range.

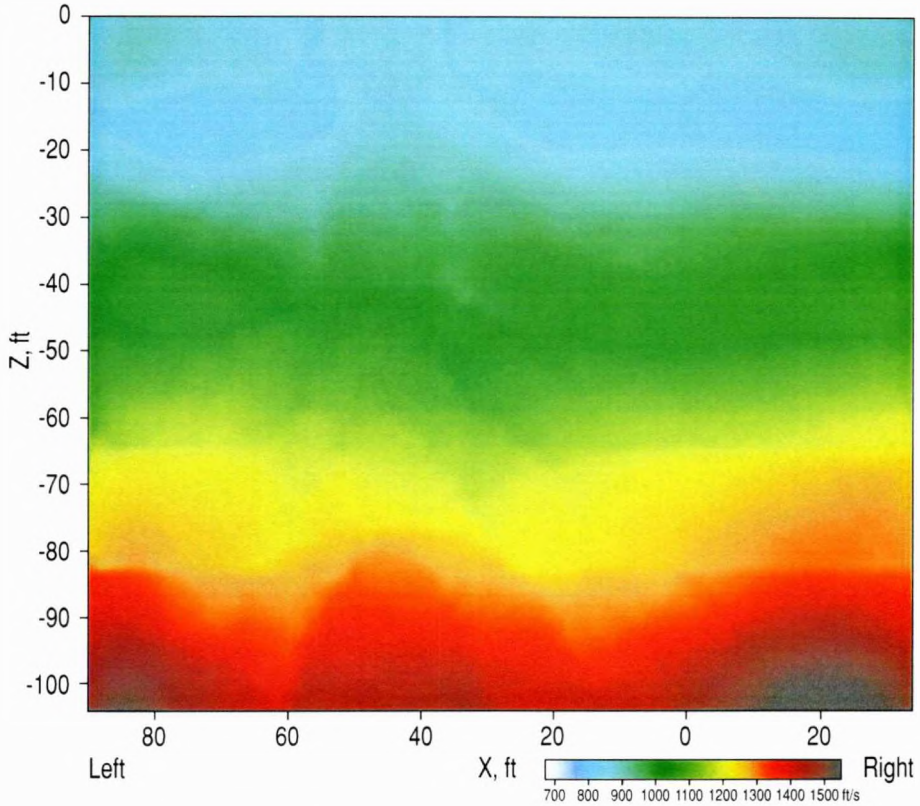

Figure 30. Clearwater Dam, Line C6, Vs, ft/s, 6-21 Hz frequency range.

to 140 ft (Figure 31). Line P2 has reflections that can be interpreted from about 60 to 70 ms down to around 90 ms, translating to a depth of between 40 ft and 120 ft below ground surface (Figure 32). This difference is related to source offset and therefore sampling of reflection points from uniquely different portions of the dam's internal structure.

Data quality and resolution potential along line P1 are very good with coherent reflections returning from within the pervious fill and core/alluvium that possess dominant frequencies from 100 Hz to over 200 Hz (Figure 31). An obvious change in reflection characteristics marks the top of the inclined core at about 80 ms. Reflections from the top of the inclined core are very irregular in geometry and coherency, seeming to imply a lack of uniformity in the pervious fill/core contact. Considering where the subsurface sampling points are for this line, some of this disturbed-looking surface is likely a result of smear along the upstream face of the inclined core and the upstream toe of core wedge (Figure 33). With the reflection wavelet having a horizontal dimension that exceeds 50 ft, each reflection wavelet returning from the core surface is actually the average of not only the CMP on the sampling plane, but also information from points all along the core wedge and the 1-to-1 slope of the clay core above the top of the alluvium across the entire 50+ ft sampling area. The wide sampling area effectively smears the information returning in the reflection wavelet so all the features within about a 50 ft circle around the reflecting point will be averaged into the reflection wavelet recorded from a particular CMP. With this resolution limitation in mind, distinguishing breaks in reflection coherency related to failure from artifacts related to non-uniform construction practices is very difficult.

Three areas can be identified on line P1 with reflection geometries that imply subsidence and therefore reduced compaction of the fill (Figure 34). Most significant is the apparent subsidence, mapped through reflection droop, that originates beneath the sinkhole and angles to the right through the pervious fill and clay core, ending at the top of bedrock where reduced amplitudes and scattered seismic energy suggest fracturing. This is clearly the most pronounced and likely candidate volume possibly representing the "root" of the sinkhole. Another volume that appears to have reflection geometries consistent with the subsurface model of subsidence features is about 30 ft left of the sinkhole and can be described as a relatively narrow chimney-like feature that appears to correlate to a section of the bedrock characterized by disturbed reflections with reduced coherency, signal-to-noise, and minor scattering. This feature does not have a direct tie to the sinkhole location nor to the trenching that was done to over 20 ft tracking the sinkhole into the subsurface. A third and final area with unusual reflection geometries is about 130 ft right of the sinkhole and appears to be a construction remnant. It relates to an area of the core (based on reflections) that possesses some sag, similar in nature to those observed beneath gradual subsidence features.

Key to the suggestion that the sinkhole "root" follows the right subsidence path is the apparent dip and offset of the 80 ms reflection beneath station 40 to 80 right of sinkhole. Most irregular reflection geometries below the dominant reflection event at around 80 ms are interpreted to be either within the native alluvium or related to construction. This suggestion is made after consideration of the material strength of the sediments that compose the dam. If these steeply dipping events were the result of subsidence, the overlying 80 ms event that is interpreted to be the top of the core wedge would be bridging a very large void or highly undercompacted area. It is very unlikely any material within the dam or alluvium has the strength to bridge across the 120+ ft necessary for the apparent structures between 85 ms and 105 ms beneath station 80

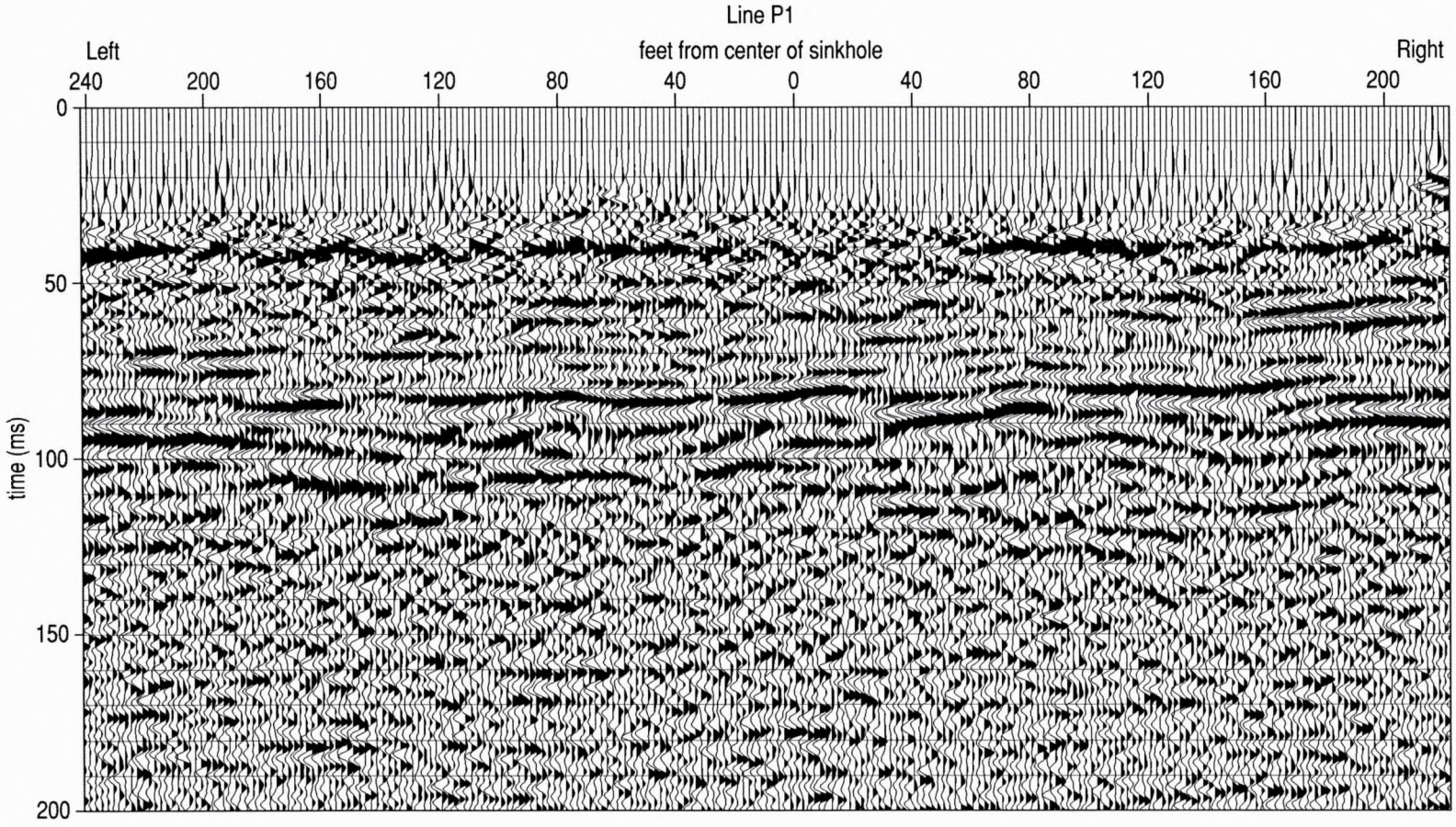

Figure 31. CMP stacked section from line P1. Reflections from the alluvium/clay core contact with the pervious fill is evidenced by the dramatic change in reflection character at about 80 ms.

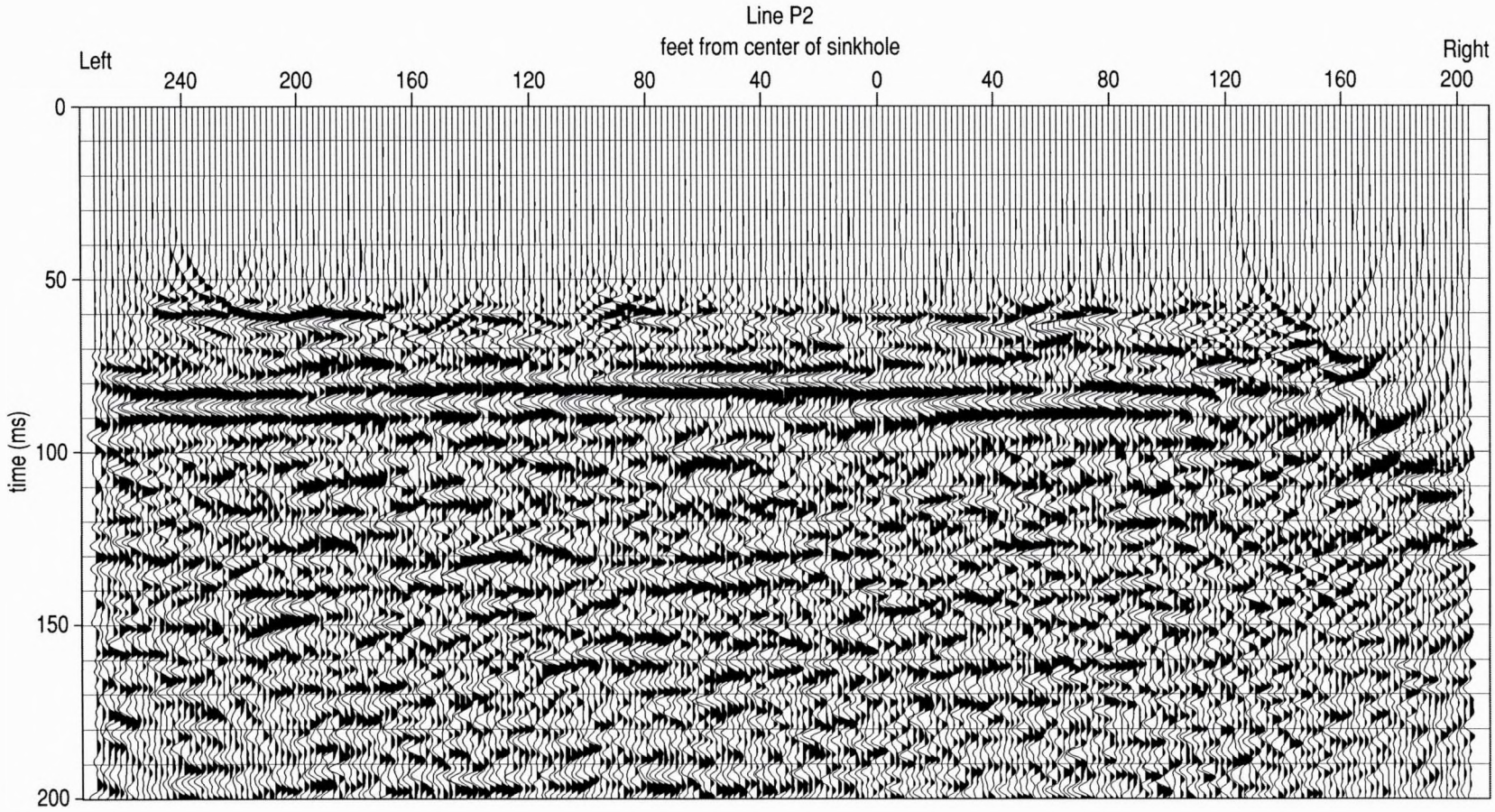

Figure 32. CMP stacked section from line P2. Reflections from the alluvium/clay core contact with the pervious fill is evidenced by the dramatic change in reflection character at about 80 ms.

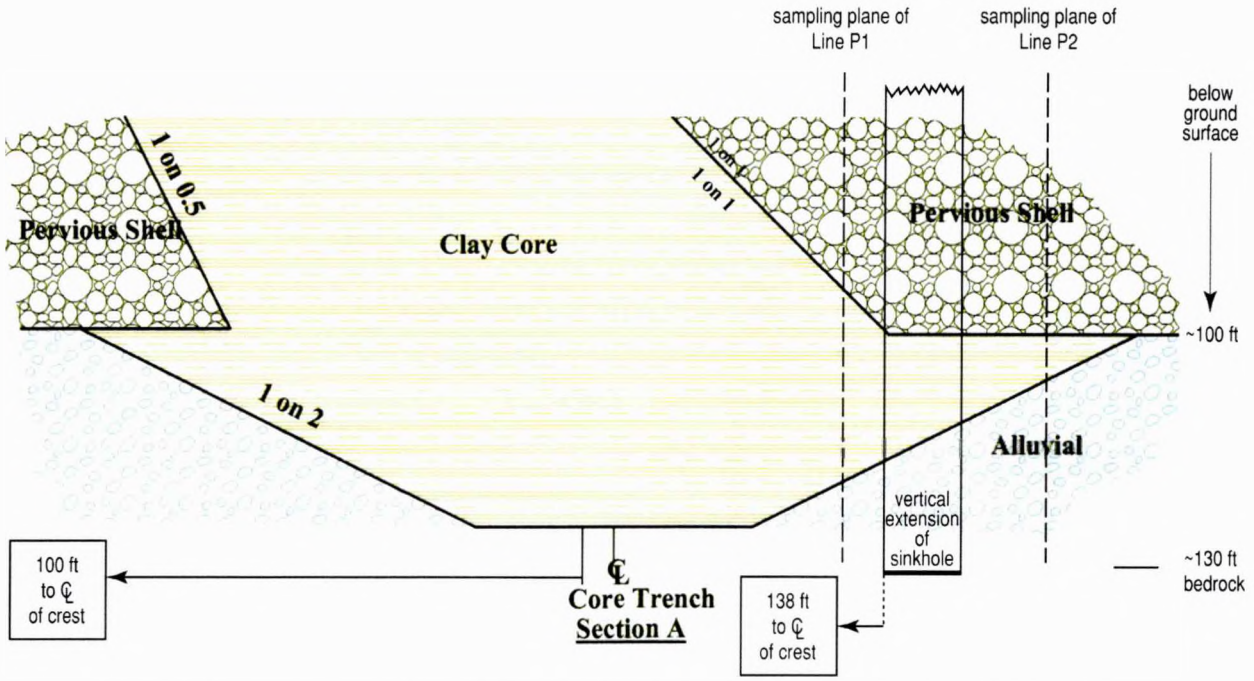

Figure 33. Dam cross-section diagramming the subsurface sampling plane for lines P1 and P2.

left to be the result of recent subsidence. The continuous layer at about 80 ms would represent the "roof rock" of such a subsidence feature and that does not seem possible considering this layer is identified as the top of the core wedge.

Beneath station 40 ft right is the most notable offset in the interpreted top of the core wedge. Above and below this offset, reflection events seem to diminish, creating a shadow zone (or zone without reflection returns) possibly indicative of a rubble zone, undercompacted area, void, or construction anomaly (dam materials were placed in piles rather than layers). Only three locations along this profile possess related features with vertical correlations of this type. These are beneath station 40 ft left, approximately 40 ft right, and 150 ft right. All have chaotic zones, reflection void zones, reflection offset or drape, and/or dipping reflections consistent with subsidence features. The two most likely candidate volumes responsible for the sinkhole are located between 40 ft and 80 ft right of the sinkhole and 30 ft to 50 ft left of the sinkhole.

One more area on line P1 that bears monitoring and possibly further investigation is located within what is interpreted as the core wedge between the sinkhole and about 120 ft left of the sinkhole (Figure 34). This zone is characterized by lower frequency and highly undulating reflection events. Considering the size of the horizontal sampling zone, it is not possible to say definitely that this unusual character is due to reduced competence or if this is a construction artifact associated with the apparent trouble that was experienced in grouting the enlarged joints and retaining the integrity of the core trench. However, until an invasive sample is taken, it will not be possible to further constrain the interpretation.

Moving away from the 1-to-1 sloping surface of the upstream clay core, reflections on line P2 are much more uniform and coherent across the profile (Figure 35). As on line P1, the reflection from the top of the core wedge is markedly different in character than the reflection

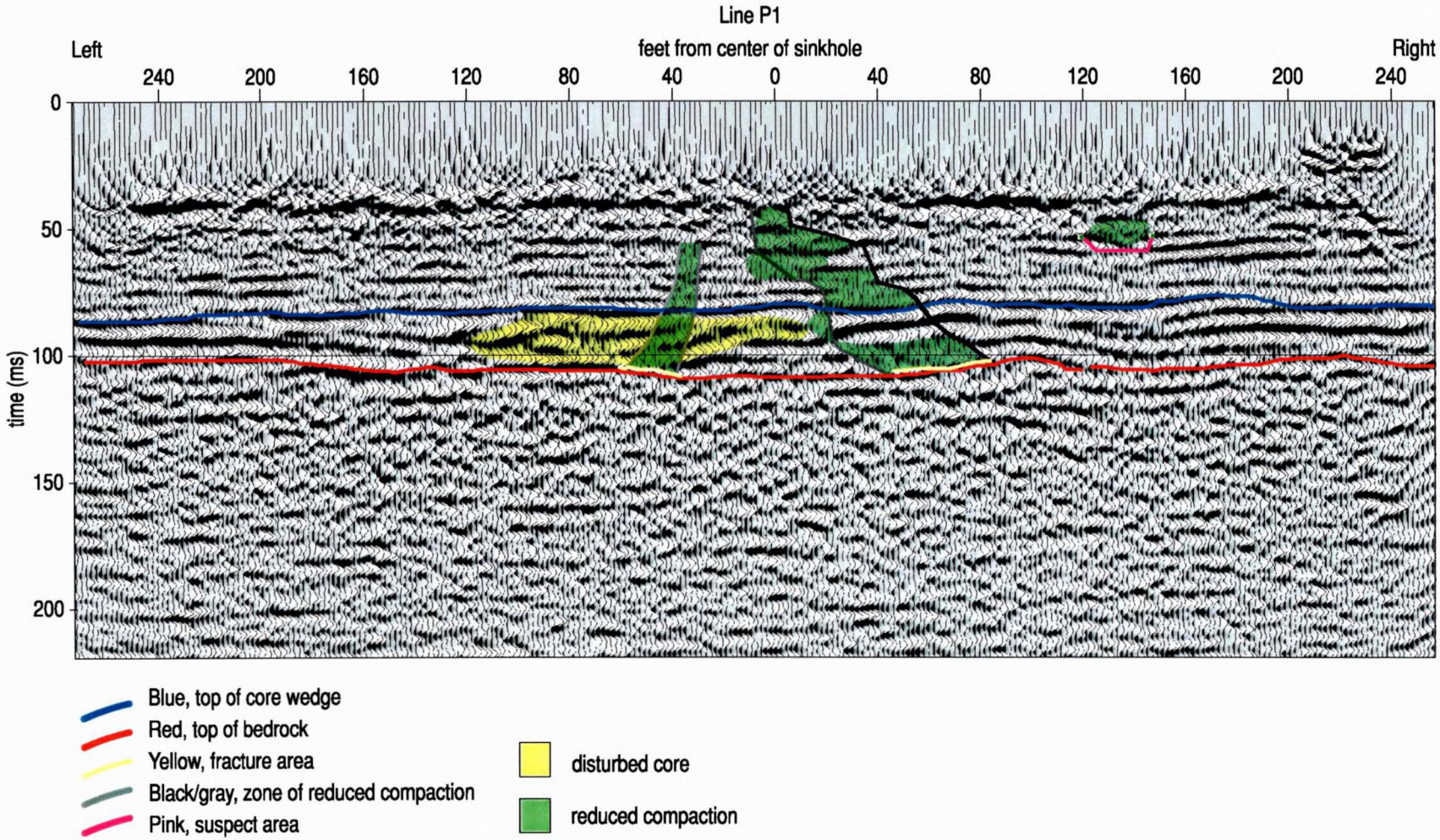

Figure 34. Interpreted CMP stack of line P1 showing key layers and abnormalities.

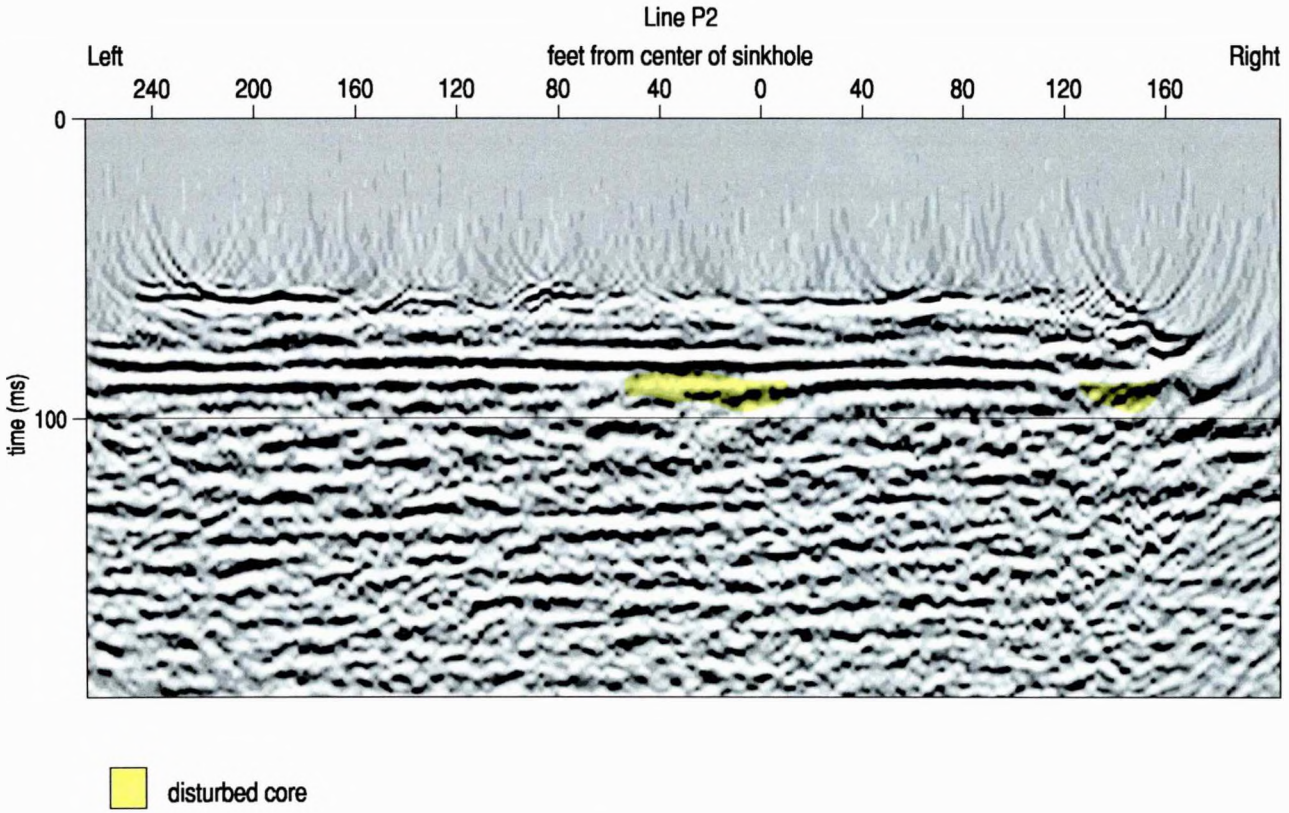

Figure 35. Interpreted CMP stacked section of line P2 highlighting areas below the top of the clay core that appear irregular.

from within the pervious fill. Evident from the subsurface sampling plane of line P2 (Figure 33) the majority of the horizontal sampling area on the surface of the clay core is on top of the core wedge and significantly away from the 1-to-1 slope of the impervious core. Reflection from within the pervious fill are high frequency and relatively coherent across the section. A few minor variations in the wavelet characteristics can be observed at about 70 ms, between about 40 ft and 120 ft right of the sinkhole. This could be related to the sinkhole or inconsistencies in compaction and fill material associated with construction. Two pronounced seismic features on the CMP stacked section of line P2 are clear: one is the drop in reflection amplitude and wave-form consistency between the center of the sinkhole and 80 ft left at about 90 ms, and the other is the dramatic change in reflection coherency and signal-to-noise between 120 ft and further to the right of the sinkhole at between 80 and 100 ms. These two features have characteristics and locations that most likely correlate with similar features observed on line P1 and with existing surface and subsurface data.

Considering the apparent competence of the inclined core/pervious fill contact along line P2, the loss of reflections immediately left of the sinkhole below the top of the inclined core is likely related to construction problems encountered while dental concreting the enlarged joints mapped immediately downstream of this feature (Figure 35). About 100 ft right of the sinkhole in an area that could represent the linear extension of bedrock fractures interpreted on line P1, the data quality drops dramatically and could be related to end of the line effects or disturbed core. These two areas on line P2 are the most obvious candidates for subsidence potential or remnants of previous subsidence or construction artifacts.

Merging the interpretations of the seismic reflection data together, looking specifically at depth ranges where disturbed material appears to be present beneath the profiles, a strong correlation can be made between the enlarged joint patterns mapped during construction of the cutoff trench and apparent bedrock fractures on seismic data (Figure 36). Line P1 is located above a very rapidly changing part of the dam where the inclined core goes from a 45 degree slope to horizontal; therefore separating construction artifacts or native layering in alluvial materials from subsidence/dissolution features is not straightforward. However, it appears the interpreted areas with bedrock alterations are consistent with the projection of the enlarged joints mapped in the core trench. It is also interesting that the base of the core wedge is disturbed in a pattern very similar to the extrapolated extension of the enlarged joints across both lines P1 and P2. This suggests possible problems during dam construction stabilizing the cutoff trench walls within the alluvium above these joints. As well, seepage through or beneath the cut-off trench associated with these enlarged joints would result in a similar image. Another possibility is a breech in the confinement at the bedrock surface resulting in vertical water movement into deeper fractures, allowing erosion within the alluvium followed by subsidence. Both features with apparent vertically disturbed zones on seismic data are directly above the upstream projections of the enlarged joints. Investigations are underway on the right side, since that seems to have been the area responsible for the current sinkhole; however, some risk does exist left of the sinkhole for future subsidence.

By combining the interpretations of all the seismic data, it appears that the sinkhole formed as a result of dissolution/erosion of materials right of the sinkhole itself, following a path that leads to the horizontal extension of the known enlarged joint pattern. Two chimney features exist from reflection data, both 30 ft to 50 ft offset from the sinkhole itself, one right and one left.

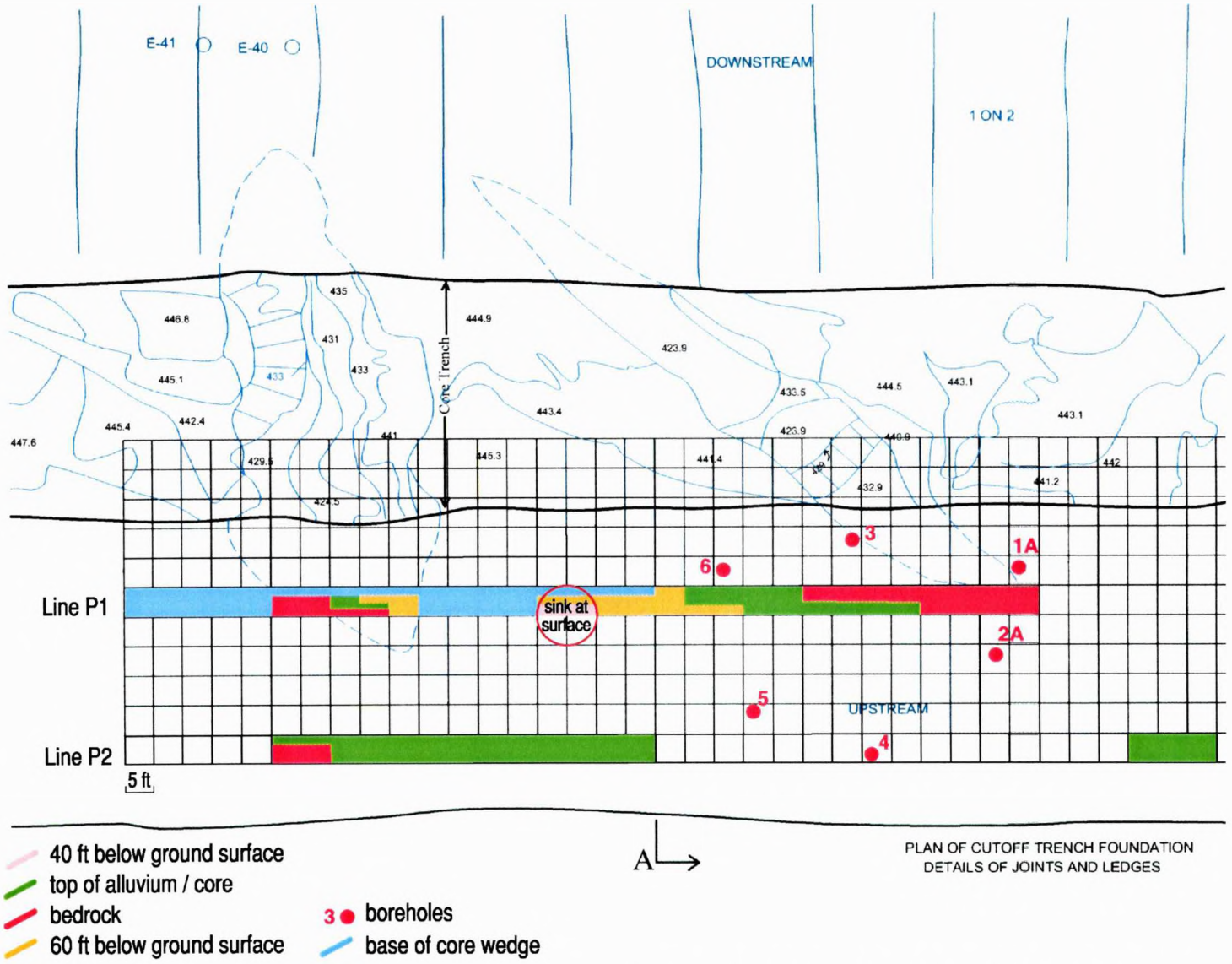

Figure 36. Map view of areas identified on reflection sections as anomalous or disturbed, possibly related to the sinkhole. The drill pattern that will be used for the cross-hole seismic survey is also shown.

Surface wave data favor the sinkhole root trending to the right. It is therefore imperative to find the path fluids took when moving sediment out of the dam interior and downstream if there is any hope of effectively remediating the structure. A cross-hole seismic survey has been designed to investigate the apparent fractures observed on seismic reflection data on the bedrock surface (Figure 36). Design of the hole pattern determines the area of investigation and resolution of the resulting data. Based on the seismic and construction data a six-hole pattern has been installed that encircles the area defined on seismic data as possessing disturbed (interpreted as fractured) bedrock. Construction materials (neat grout and placed clay layers) were encountered in two of these boreholes where they were not expected. These unexpected encounters imply that the core trench was likely much larger in this area than planned and possibly responsible for some of the irregular reflection arrivals interpreted as disturbed materials.

Interpretation of materials the borings encountered include concrete above bedrock and a river gravel in SH-1A and two placed clay layers inside the alluvial zone and neat grout just above rock in SH-5 (Hartung, personal communication) (Figure 36). These abnormalities are indicative of real-time fixes to problems encountered during construction but not reported in any known surviving documentation. If these materials are laterally continuous across distances as short as a few 10s of feet they could produce reflections with irregular wavelet attributes, possess characteristics potentially indicative of subsidence (droop, amplitude variability, extreme dips, etc.), and would be difficult to correlate with dam designs and therefore assumed related to changes in internal dam structure since construction.

Discussion

It appears from the two data sets that the narrow "chimney" that has been observed to depth in excess of 20 ft through vertical trenching is significantly wider below about 30 or 40 ft from the ground surface and trends to the right along a narrow finger-like corridor. This elongated to the right and very irregular pattern is for the most part associated with a predominantly vertical meander pattern. The overall seismic data quality appears excellent with greater penetration of the surface wave data than expected and shallower imaging with the P-wave data than planned. Disturbed bedrock and dam materials are interpretable on seismic data and provide insight into the mechanism responsible for the removal of sediment and eventual subsidence within the dam.

Surface wave analysis—
Data from the shallow portion of the sections (upper 15 ft) is not nearly as accurate as was planned. For the most part this is due to the presence of the sinkhole and its affect on wave propagation associated with the 25 Hz to 60 Hz frequency band. The deeper data, however, does possess very good signal-to-noise and therefore equally as good convergence to a solution.

Line C2 has some indications of a lower velocity but not particularly unique near surface on these data as can be seen from a similar low velocity zone (white on the plots) near the left end of the profile. Near the center of the sinkhole there does not appear to be any unique indications of lower velocity material expected as indicative of the chimney discovered during trenching.

Line C3 is probably the banner line in terms of imaging the chimney most clearly and with the greatest resolution. The sinkhole is sufficiently small that, in combination with the missing high frequency portion of the surface wave spectrum, the seismic expression of the sinkhole above about 35 ft or so is not represented by a strong velocity gradient as expected; however, below about 40 to 45 ft the sinkhole becomes quite obvious. It extends from about 10 ft left of the sinkhole to 30 ft right of the surface depression around 70 ft below ground surface. Considering the averaging effects associated with this kind of imaging, the subsidence volume is not likely uniform in terms of stiffness or compaction. This zone of reduced shear wave velocity is probably more of a series of collapse meanders that change direction and follow zones of least strength.

Line C4 provides a similar picture to that seen on line C2, but much smaller in physical dimensions. A low shear velocity zone between 14 ft left and 16 ft right of the sinkhole is the chimney structure or strength-altered zone. Clearly the sinkhole expression has reduced in size in the subsurface by about half across the 8 ft that separates lines C4 and C3. The low velocity is still pronounced but does not have quite the velocity gradient observed on C3 likely as a result of the horizontal averaging between all the rocks within the spread length.

Lines C5 and C6 have subtle undulations in the velocity along the profiles at around 60 to 80 ft below ground surface, but none of these variations in velocity rise above the background or normal fluctuations expected in data from this setting.

In summary, from the surface wave data it appears that the chimney is elongated to the right and possesses a sizeable footprint at depths below about 45 ft. It does not seem to extend significantly upstream or downstream beyond C2 or C4 (16 ft zone). However, if this chimney diverts along a small seam of lower strength or a less resistant zone (fingering) the reduced strength or subsidence volume could extend upstream or downstream along a path that is below the resolution of this survey.

P-wave reflection data—

The reflection data were excellent and much better than expected. With upper corner frequencies extending well beyond 300 Hz the data resolution was sufficient to allow the detection of layering within the dam shell material (pervious fill), likely indicative of the layering and compaction sequences used during construction. This higher than expected resolution also allows the expression of the sinkhole to be tracked from about 40 ft below the ground surface down to the top of bedrock with unusual accuracy and associated confidence.

Starting at the top of the section beneath the sinkhole, a downdropped reflection can be seen at about 50 ms, which equates to about 45 ft. This zone is about 15 ft wide and extends from about station 8 ft right to 8 ft left of the sinkhole, then from here there are two possible scenarios: it appears to drift abruptly to the right side, or possibly gently to the left side. If the right path is followed, at about 70 ft it appears to widen from 10 ft left of the sinkhole to over 40 ft right of the sinkhole. Looking deeper into the section the "chimney" or subsidence-altered zone appears to meander around stronger or more resistant layers, with these stronger layers forming bridges or in some cases subsiding intact. At or near the top of the inclined core, interpreted at about 80 ms (~100 ft), a reflective layer appears offset a bit. This offset is unique to these data and the principal evidence to suggest the right subsidence path is the most probable. The void or less

competent volume traceable in the subsurface continues to move right and at the bedrock surface correlates with a set of what appear to be fractures located between 80 ft and 20 ft right of the sinkhole. These inferred fractures correlated quite closely to the projection of the enlarged joints observed during dam construction.

The right path matches the surface wave data best, but the left path must also be considered due to the well-defined nature and vertically consistent disturbed zone appearing to tie to the sinkhole. A narrow zone void of reflections is interpretable between 50 ms and the interpreted top of the core wedge (Figure 34). This disturbed volume is very consistent, from a geometric perspective, with the excavated portion of the sinkhole above 25 ft below ground surface. The near-vertical nature is also a better fit with the soil mechanics likely controlling this structure. However, the right void/subsidence pattern has better ties with the center of the sinkhole and has much better defined lost-reflection zones that are identified as collapse volumes. The left subsidence feature appears to be a true anomaly with this dam structure and does correlate to a known enlarged joint.

This area of concern forming left of the current sinkhole needs to be investigated invasively to ascertain the physical changes in the dam structures as detected on the seismic data. This near-vertical zone of disturbed material can be traced down to the bedrock where a fracture zone has been interpreted. This interpreted bedrock fracture is consistent with one of the enlarged joints observed and dental concreted during dam construction. Currently this second zone of altered reflections appears to have only moved to within about 60 to 70 ft of the surface. However, considering its strong expression within the pervious fill material, it should be considered a strong candidate for continued vertical movement, with a reasonable possibility it will eventually result in a surface depression.

Two scenarios appear possible: 1) much of the disturbed material is related to construction artifacts and the sinkhole is a result of erosion by water moving vertically into bedrock upstream of the core, or 2) the core is breeched at or near the enlarged joints and seepage at the base of the core provides the conduit for moving sediment out of the dam. It is very unlikely the highly altered area on seismic data left of the sinkhole (identified as disturbed core on Figure 34) is a result of recent subsidence. Considering materials strengths, this much collapse would have migrated rapidly to the dam surface.

APPENDIX A

Basic principles and concepts of practical shallow seismic reflection profiling

D.W. Steeples and R.D. Miller

Abstract — *Seismic reflection is a powerful geophysical exploration method that has been in widespread use in the petroleum industry for more than 60 years. This paper addresses some basic principles of the method and its application at depths shallower than 30 m (100 ft). Since 1980, the shallow reflection technique has been increasingly used for engineering and environmental problems, such as mapping bedrock beneath alluvium and delineating intra-alluvial features near hazardous waste sites, detecting voids in coal and karst, defining the top of the saturated zone and mapping shallow faults. New applications will be added with improved resolution and increased cost-effectiveness.*

Introduction

This paper describes some of the basic principles of seismic reflection and their significance, as applied to shallow engineering, mining and environmental projects. The seismic reflection method is a powerful technique for underground exploration that has been in use since the 1920s (Waters, 1987; Dobrin, 1976; Coffeen, 1978; Telford et al., 1976; Sheriff, 1978). The use of seismic reflection surveys for imaging targets shallower than 30 m (100 ft) has only been available since the early 1980s. The technique is finding new applications in characterizing the geologic, hydrologic and stratigraphic conditions within 3 to 30 m (10 to 100 ft) of the earth's surface. As research and development continues, higher and higher seismic frequencies will be attainable, allowing practical prospecting for progressively smaller geologic targets.

Seismic reflection techniques depend on the existence of discrete seismic velocity and/or mass density changes in the subsurface, known as acoustic impedance contrasts. Mathematically, acoustic impedance is simply the product of mass density and acoustic wave velocity. Acoustic impedance contrasts occur at natural boundaries between geologic layers, although manmade boundaries, such as tunnels and mines, also represent contrasts. The classic use of seismic reflection is to identify the boundaries of layered geologic units. However, the technique can also be used to search for localized anomalies such as sand/clay lenses and cavities.

Compressional waves (P-waves) propagating through the earth behave similarly to sound waves propagating in air. When sound waves (voices, explosions, horns, etc.) come in contact with a wall, cliff or building (all acoustic contrasts), it is common to hear an echo. When a P-wave comes in contact with an acoustical contrast underground, echoes (reflections) are also generated. P-wave reflections can be thought of as sound wave echoes from underground acoustic impedance contrasts. In the underground environment, the situation is more complex because some P-wave energy impinging on a solid acoustical interface can also be transmitted across the interface, refracted at the interface and/or converted to other types of seismic waves at the interface.

Seismic methods are sensitive to the physical properties of earth materials and relatively insensitive to the chemical makeup of contained fluids in earth materials. Electrical methods are sensitive to contained fluids and to the presence of magnetic or electrically conductive materials. The measurable physical parameters upon which the seismic methods depend are quite different from the important physical parameters for electrical and magnetic methods. In the world of shallow geophysics, there are similarities among seismic reflection, seismic refraction and ground-penetrating radar. There are also similarities with cross-hole seismic tomography and vertical seismic profiling. The similarities with electrical and potential fields methods are substantially less.

The work of Hunter and Pullan and their colleagues at the Geological Survey of Canada (Hunter et al., 1984; Pullan and Hunter, 1985) and Helbig (Doornenbal and Helbig, 1983; Jongerius and Helbig, 1988) and his students at the University of Utrecht in The Netherlands has been instrumental in developing shallow seismic reflection techniques. In particular, the simple data manipulation and display of Hunter's optimum window-common offset makes it a cost-effective method of imaging the shallow subsurface in areas conducive to seismic reflection.

Shallow seismic reflection fundamentals

The simplest case of seismic reflection is a single layer over an infinitely thick medium (Fig. 1). Seismic energy induced into the ground from a point is radiated spherically away from that point in much the same fashion in three dimensions as waves from a pebble tossed into a still pond radiate outward in two dimensions (Fig. 2). An arbitrarily large number of ray paths can be traced outward from the seismic energy source. One particular ray path will direct energy to a subsurface layer, reflect from that subsurface layer and return as an echo to the ground surface first,

D.W. Steeples, member SME, and **R.D. Miller** are associate research director and assistant scientist, respectively, with the Kansas Geological Survey, University of Kansas, Lawrence, KS. SME nonmeeting paper 91-207 B. Manuscript Feb. 22, 1991. Discussion of this peer-reviewed and approved paper is invited and must be submitted, in duplicate, prior to Dec. 31, 1993.

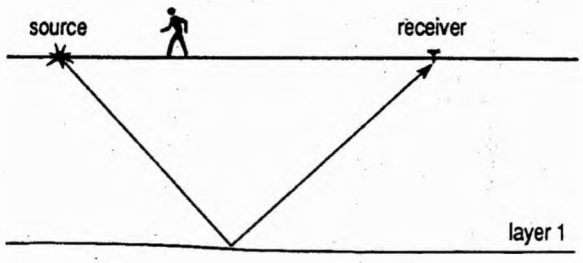

Fig. 1 — Reflection from one subsurface layer. The angle of incidence of the downgoing ray is equal to the angle of reflectance of the upgoing ray.

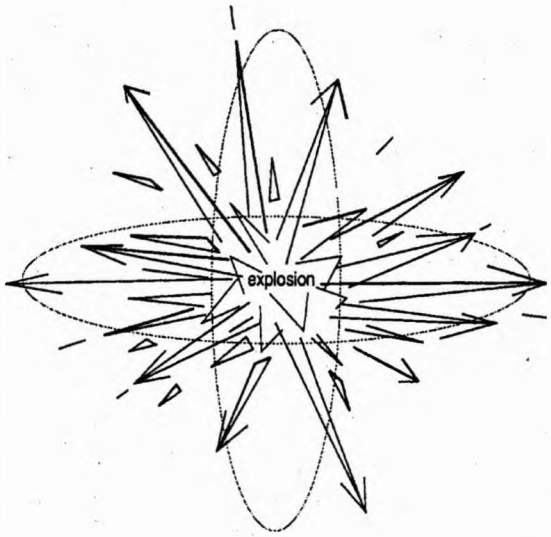

Fig. 2 — Computer simulation of energy radiating out from a subsurface explosion.

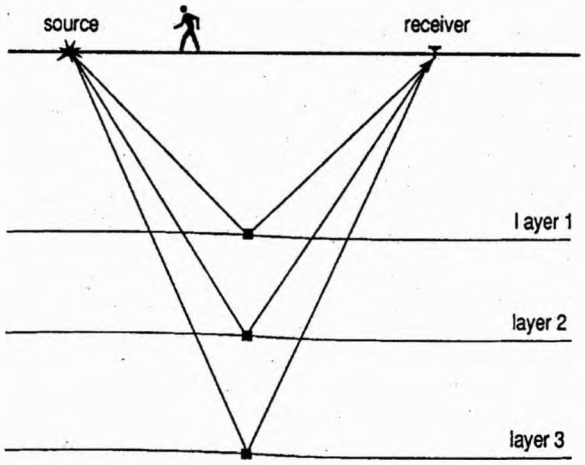

Fig. 3 — Reflection from three subsurface layers. The angle of incidence is different for each layer/ray but the reflecting points are vertically equivalent.

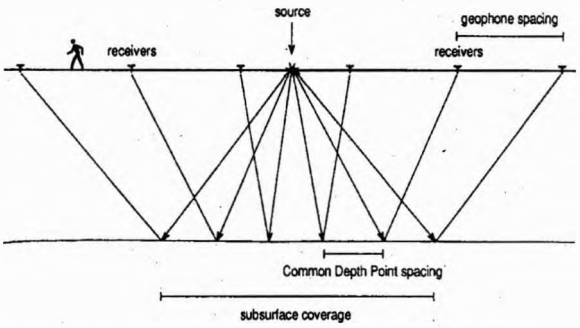

Fig. 4 — Schematic of seismic ray paths for a single shot with a six-channel reflection seismograph.

following Fermat's principle of least travel time. In the case of a single, flat-lying layer and a flat topographic surface (Fig. 1), the path of least time will be from the energy source to a reflecting point midway between the source and the receiver, and then back to the receiver. The incident angle of the down-going ray will be equal to the angle of reflection of the upgoing ray from the subsurface layer.

Several layers beneath the earth's surface are commonly targeted by a single seismic reflection survey (Fig. 3). Seismic data are more complex when several layers are involved. Seismic energy can be converted from one wave type to another at layer interfaces. The simple, one-layer case (Fig. 1) becomes slightly more complicated when considering all the possible raypaths and wave conversions. The apparent complexity of a seismogram directly relates to the variety of types of seismic waves and their associated characteristic velocities and travel paths. Complexity is often increased as well by the presence of seismic energy that has bounced more than one time off layers in the subsurface (multiple reflections). Reflected energy from successively deeper and deeper boundaries appears on a seismic trace at greater and greater time.

Expanding the multilayer case of Fig. 3 to multiple receivers allows travel path vs. arrival time determinations and comparisons (Fig. 4). Rays reflected from different points in the subsurface are recorded by receivers appropriately spaced on the ground surface. The distance between these subsurface reflecting points is exactly half the distance between receivers, providing a closer subsurface sampling interval than the surface receiver spacing. The recording of multiple receiver-channel locations for each individual shot allows determinations of apparent velocity (travel path-arrival time) and apparent reflector dip.

Source and receiver locations can be placed so that path S1-R2 reflects from the same location in the subsurface as path S2-R1 (Fig. 5). The subsurface point that is in common for both source and receiver pairs is called a common reflection point (CRP) (Mayne, 1962), a common depth point (CDP) or a common midpoint (CMP), depending on the preference of the author (Fig. 5).

The power of the CDP method is in the redundancy in sampling of a particular subsurface location. By gathering traces in a computer according to CMP and time-adjusting them for different travel-path lengths, traces with the same CMP can be added to enhance the reflection signal. The degree of redundancy or multiplicity of data at a particular

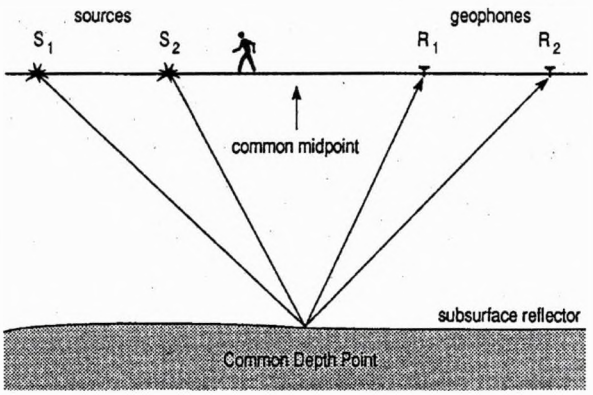

Fig. 5 — The concept of common depth point (CDP). Note that ray paths from two different shots (Sl and S2) reflect from a common point in the subsurface.

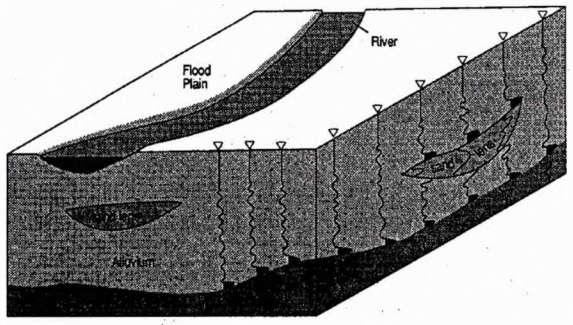

Fig. 6 — Schematic showing a seismic section relating to real-world geology.

point is known as "CDP fold." A 24-channel seismograph, for example, is typically used to gather 12-fold CDP data. From a theoretical standpoint, signal-to-noise ratio of reflections improves proportionally to the square root of the CDP fold. For shallow reflection data in particular, it is important to remember that one-fold of good data is better than many-fold of bad or marginal data.

The seismic reflection method is generally used to determine the spatial configuration of underground geological interfaces. Displaying all the CDP stacked traces consistent with their spatial locations results in a reflection-time cross-section of a portion of the earth (Fig. 6). The peaks of the seismic reflections (wiggles) are generally blackened to assist in interpretation. This schematic example (Fig. 6) is a very simple version of typical near-surface geology that depicts a buried sand lens in a river valley. Resolving a fixed-size target becomes more difficult with increasing depth below the ground surface, but the physical principles remain the same. Resolving power is a linear function of increasing the frequency and bandwidth of the seismic reflection data.

Obtaining high quality shallow seismic reflection data is still somewhat of an art, where an individual's ability improves with experience. Improving the quality of shallow reflection data depends on careful, meticulous procedures based on sound scientific observation and theory, step-by-step data analysis, stringent quality control during all aspects and avoiding invalid assumptions during the acquisition, processing and interpretation of shallow reflection data.

Practical shallow reflection surveying

Seismic reflection surveys routinely involve three basic parts: acquisition, processing and interpretation. A variety of selectable parameters and methods are possible at each of these three distinct stages. Pronounced differences exist between shallow and conventional seismic reflection techniques during the acquisition and processing stages. The basic principles of interpretation for shallow and conventional seismic reflection are consistent, except for scale differences. The underlying theoretical basis for the seismic reflection method is consistent for conventional and shallow applications.

Acquisition

The basic instrument for seismic studies is a seismograph, which is analogous to a stereo music system. The better the music system, the more detail the listener can ascertain from subtle background instruments. Likewise, the better a seismograph's dynamic range, the more the potential for distinguishing subtle geologic features. A stereo music system has variable controls to enhance high frequencies (like a flute) or low frequencies (like a tuba). A seismograph has similar selective capabilities for emphasizing recorded sound frequencies. A seismograph that can record and enhance high frequency sound waves is necessary to detect small geologic features. The use of high frequency seismic waves (>80 Hz) in reflection seismology is known as "high resolution" seismic exploration (Sheriff, 1991).

A stereo system also has an amplifier volume control where a seismograph has amplifier gain control, either fixed (selectable) or floating point (automatic). Selection of the frequencies to be enhanced and the amplifier gain necessary to maximize the recorded relevant geologic information depends on the depth and size of the underground geologic features of interest and the acoustic properties of the near-surface material.

Receivers for detecting reflected acoustic signals in the ground are called geophones. These are very specialized microphones similar in principle to those used in voice recording. The operation of a geophone is based on the voltage induced in a coil of wire when it moves through a magnetic field. For most geophones, a magnet is rigidly attached within the geophone case. A coil of wire mounted on a spring surrounds the magnet. When the case experiences movement, the coil moves relative to the magnetic field (set up by the magnet), which in turn induces a voltage proportional to the velocity of the ground motion. Selection of the appropriate geophone for a particular survey should be based on dominant frequency and amplitude of the signal.

The most site-dependent part of the acquisition system is the acoustic energy source. A variety of sources have been developed and are in routine use on shallow seismic reflection projects. As a human voice is a source of acoustic energy, so is an explosion, a book dropped onto the floor, a car horn or an electric razor. The method of generating and transmitting acoustic energy into the ground is what determines the quality of a source at any particular site.

There are two types of sources: impulsive and vibratory. Impulsive sources are the predominant type of shallow seismic source while vibratory sources are the predominant conventional seismic source. The frequency-limited nature

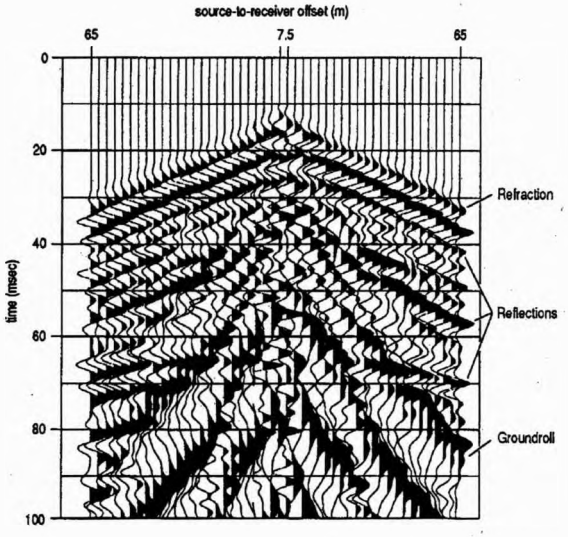

Fig. 7 — 48-channel field file acquired in a split-spread format. The source is located between two sets of 24 channels.

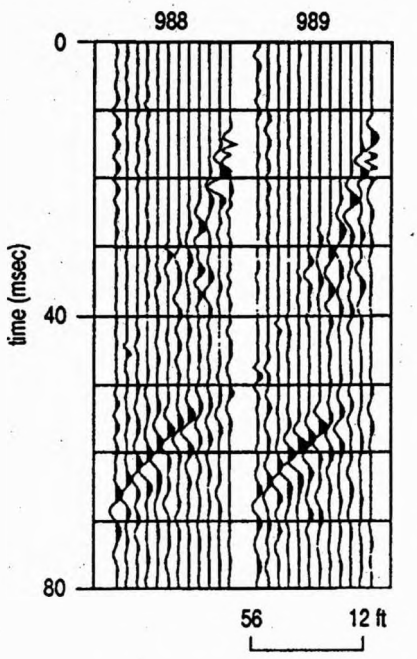

Fig. 8 — Two CDP gathers from a 24-channel seismograph. The hyperbolic curvature of the reflection arrival is easily identified.

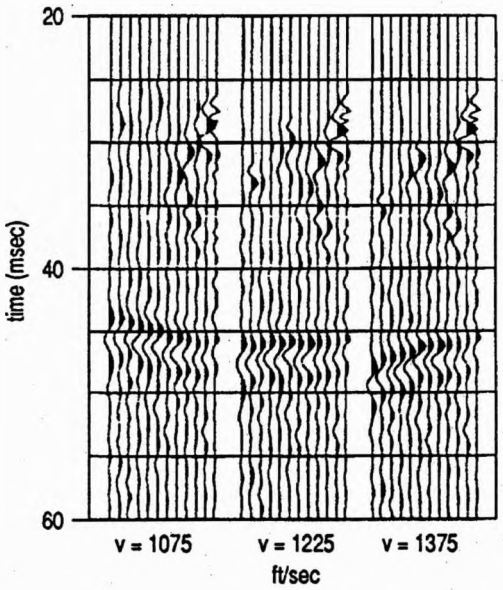

Fig. 9 — CDP gathers from Fig. 8 moved out at various velocities.

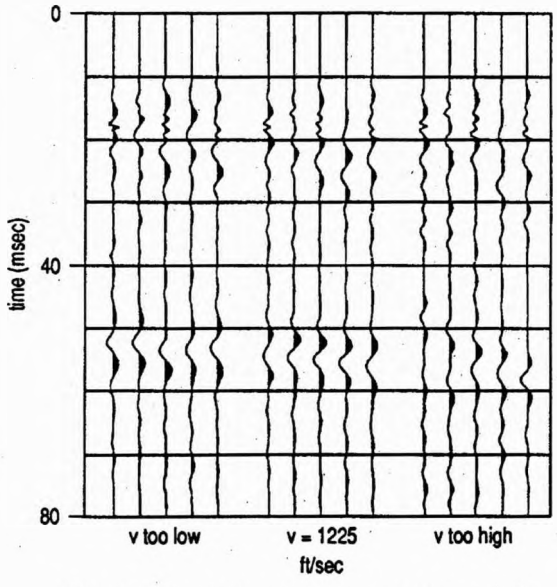

Fig. 10 — The effects of an improper stacking velocity.

of vibratory sources is what has held them to very limited used on shallow reflection surveys. Most shallow reflection surveys employ weight drop (accelerated) or explosives as the source of acoustic energy.

Processing shallow reflection data

The purpose of acquiring and processing seismic reflection data in a CDP format is to enhance reflections at the expense of everything else. There are a variety of filtering, display and static correction techniques that can be employed to improve the quality of the reflections. Discussion here is limited to only those techniques that are necessary to understand the fundamentals of CDP processing. There are many places in the scientific literature to obtain more details (Waters, 1987; Yilmaz, 1987; Robinson and Treitel, 1980).

Raw seismic data are in a field file or shot gather format, with each seismograph channel or seismic trace for a particular shot ordered according to channel number (Fig. 7). The number of seismic traces within each shot gather is equal to the total number of seismograph channels. Before gathering or sorting the data into a CDP format, dead or unacceptably noisy traces are removed and the location of each station is defined in three dimensions. A CDP gather, from a simplistic point of view, is a collection of seismic traces that have a common midpoint in the subsurface.

Before stacking (adding) seismic traces with equivalent subsurface sample points, it is necessary to compensate for different travel-path lengths (arrival time of the reflection) and localized variability in the near-surface material. The arrival pattern of reflection wavelets across receivers with linearly increasing distance from the source is a hyperbolic function (Fig. 8). This hyperbolic arrival pattern, or normal moveout curve, is a result of the nonlinear increase in travel path for a ray traveling down to a reflector and back to the surface with a linear increasing in distance from source to receiver.

To properly correct for different ray path lengths, the average velocity above the reflector must be known (Fig. 9). The simplest procedure to determine the seismic velocity for good seismic reflection data is to fit a hyperbola (x^2,t^2) to the data. The degree of curvature of the hyperbola or normal moveout curve of the reflection arrival (assuming horizontal surfaces) is dictated by the average seismic velocity above the reflector, depth to the reflector and distance between geophones.

Once corrected, the data emulate what would be observed with zero distance between shot and geophone, known as zero-offset (vertical incidence). Proper time adjustment to correct for offset allows traces with common midpoints to be directly added without sacrificing any wavelet properties. The correct velocity gives the highest frequency and the best coherency on the stacked data (Fig. 10).

Variations in the velocity and thickness of the near-surface material cause errors known as statics, which uncorrected, can produce apparent geologic structures that have no geologic significance. Static variations are most commonly determined using cross-correlation techniques, such as surface consistent statics, residual statics, common offset statics and refraction statics. Correcting static variations is accomplished through whole-trace time shifts representative of variability in the near-surface, generally in a relatively localized area.

A variety of filtering, scaling, display and analysis techniques much less significant to the understanding of shallow data CDP processing are routinely used to improve overall data quality. The basics of CDP processing discussed here should provide a general understanding of what is most significant to the generation of high quality stacked sections.

Interpretation

Seismic reflection data can be displayed in many forms including CDP stacked section, shot gather (field file), CDP gather and common offset section. Data displayed in any of these formats have features that require special considerations when trying to interpret the significance of the wiggles.

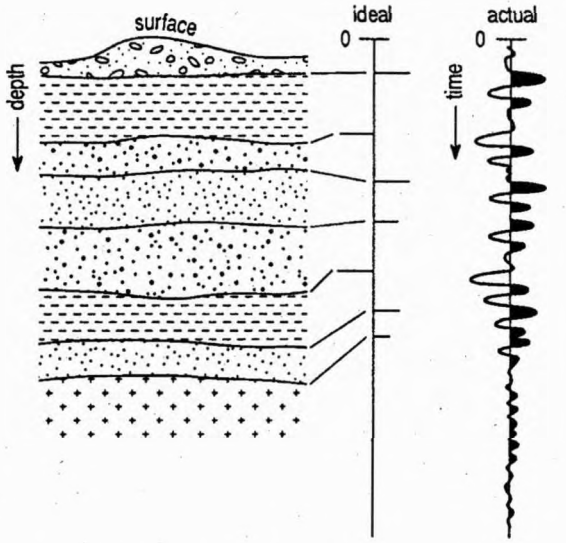

Fig. 11 — Actual seismic trace (with simulated noise) that would result from a reflection survey over the geologic model. The spike or ideal trace represents the acoustic impedance contrasts at each interface.

First, with shallow reflection data, not every wiggle necessarily has special geologic significance. Noise is present on any seismic data set, and overly optimistic interpretations that draw meaning from every wiggle will eventually lead to misinterpretations.

CDP stacked sections are corrected to represent vertically incident time arrivals . Therefore, of all the data display formats, CDP stacked data most closely equate to a geologic cross section. Common offset data are similar to CDP in the similarity to a geologic cross section. However, common offset data generally are not corrected from nonvertical travel paths. Conversions from time to depth must compensate for the increased time of arrivals.

Data in either shot gather or CDP gather format are generally ordered according to distance from shot to receiver. In this arrangement, a single reflecting interface will be recorded at ever-increasing times at longer offsets. Interpretations based on shot or CDP gathered data are generally limited to approximate reflector depths and occasionally the inference (in a qualitative sense) of faulting or dipping beds. Seismic reflection data are almost always displayed relative to two-way travel time, which can be converted in a general sense to depth if velocity is known.

Seismic reflection data in a CDP stacked or common offset format can be thought of as the time equivalent to a highway road cut where geologic units are exposed for viewing. The accuracy of the conversion of a time seismic reflection section to a depth geologic cross section depends on how well the average velocity from the surface to each reflector is known. The wiggles on a reflection seismogram represent amplitude (loudness from a sound wave perspective) of an echo that arrived at the geophone at a particular time. That time, when multiplied by the average seismic velocity within the earth, equates to twice depth. If the travel time of an acoustic pulse from the surface to a variety of depths in the subsurface can be determined from borehole geophones, conversion of time to depth can be very accurate.

If, on the other hand, no borehole seismic velocity information is available, the NMO velocity must be used to approximate depth. NMO, or stacking velocity, is always 0 to 20% greater than the real average velocity. Reflector depths estimated from NMO or stacking velocities cannot be more than 20% deeper than the actual reflecting interface.

The nature of seismic energy is responsible for the representation of recorded signal in the form of a wave (wiggle) (Fig. 11). Extracting discrete geologic boundaries or anomalies from the series of wiggles present on seismic data requires the actual or inferred removal of the source wavelet or characteristic sound of a source. Seismic data recorded using the perfect source (flat frequency spectrum from zero to infinity) have spikes that represent each acoustic imped-

ance contrast with the height of a spike directly related to the acoustic impedance contrast at the interface.

Unfortunately, since no perfect source exists, the spikes of the perfect source are spread out in time and become waves whose appearance or characteristics are related to the unique spectral properties of the actual source. The narrower the bandwidth of the source the farther from a spike and the 'ringier' the reflection wavelets become. In some cases, a reflection may be represented by a wavelet with as many as three zero crossings (three positive and three negative deflections). The interpretation of seismic data requires a good understanding and working knowledge of the source wavelet for a particular source and experience with distinguishing interference between wavelets from two closely spaced reflectors.

Conclusion

Seismic reflection is a powerful geophysical tool for exploration of the subsurface. Applications of the technique to engineering, environmental and ground water problems has only recently become cost-effective. As with any geophysical technique, as long as the basic principles and limitations are understood and no assumptions are made, shallow seismic reflection can provide subsurface continuity not possible by any other means at some locations. ♦

References

Coffeen, J.A., 1978, *Seismic exploration fundamentals*, PennWell Publishing Co., Tulsa, Okla., 277 pp.

Dobrin, M.B., 1976, *Introduction to geophysical prospecting*, McGraw-Hill Book Co., New York.

Doornenbal, J.C., and Helbig, K., 1983, "High-resolution reflection seismics on a tidal flat in the Dutch Delta-Acquisition, processing, and interpretation," *First Break*, May, pp. 9-20.

Hunter, J.A., et al., 1984, "Shallow seismic reflection mapping of the overburden-bedrock interface with the engineering seismograph — some simple techniques," *Geophysics*, Vol. 49, pp. 1381-1385.

Jongerius, P. and Helbig, K., 1988, "Onshore high-resolution seismic profiling applied to sedimentology," *Geophysics*, Vol. 53, pp. 1276-1283.

Mayne, W.H., 1962, "Horizontal data stacking techniques," supplement to *Geophysics*, Vol. 27, pp. 927-938.

Pullan, S.E., and Hunter, J.A., 1985, "Seismic model studies of the overburden-bedrock reflection," *Geophysics*, Vol. 50, pp. 1684-1688.

Robinson, E.A., and Treitel, S., 1980, *Geophysical signal analysis*, Prentice-Hall, Inc., Englewood Cliffs, N.J., 466 pp.

Sheriff, R.E., 1978, *A first course in geophysical exploration and interpretation*, International Human Resources Development Corp., Boston, 313 pp.

Sheriff, R.E., 1991, *Encyclopedic dictionary of exploration geophysics*, 3rd ed., Society of Exploration Geophysicists, Tulsa, Okla., 376 pp.

Telford, W.M., et al., 1976, *Applied geophysics*, Cambridge University Press, New York, 860 pp.

Waters, K.H., 1987, *Reflection seismology — A tool for energy resource exploration*, 3rd ed., John Wiley and Sons, New York, 538 pp.

Yilmaz, O., 1987, *Seismic data processing*; S.M. Doherty, Ed.; *Investigations in Geophysics* series, No. 2, E.B. Neitzel, Series Ed., Society of Exploration Geophysics, Tulsa, OK.

References

Batzle, M., D. Han, and J. Castagna, 1999, Fluids and frequency dependent seismic velocity of rocks [Exp. Abs.]: Soc. Explor. Geophys., p. 5-8.

Berryman, J.G., P.A. Berge, and B.P. Bonner, 1999, Role of λ-diagrams in estimating prorosity and saturation from seismic velocities [Exp. Abs.]: Soc. Explor. Geophys., p. 176-179.

Chiu, S.K.L., E.R. Kanasewich, and S. Phadke, 1986, Three-dimensional determination of structure and velocity by seismic tomography: *Geophysics*, v. 51, p. 1559-1571.

Cottin, J.F., P. Deletie, H. Jacquet-Francillon, J. Lakshmanan, Y. Lemoine, and M. Sanchez, 1986, Curved ray seismic tomography–Application to the Grand Etang Dam (Reunion Island): *First Break*, v. 4, no. 7, p. 25-30.

Glover, R.H., 1959, Techniques used in interpreting seismic data in Kansas: In *Symposium on Geophysics in Kansas*, ed. W.W. Hambleton. Kansas Geological Survey Bulletin 137, p. 225-240.

Hunter, J.A., S.E. Pullan, R.A. Burns, R.M. Gagne, and R.L. Good, 1984, Shallow seismic reflection mapping of the overburden-bedrock interface with the engineering seismograph–Some simple techniques: *Geophysics*, v. 49, p. 1381-1385.

Ivanov, J., 2002, JASR – Joint analysis of surface waves and refractions. Ph.D. dissertation, University of Kansas.

Ivanov, J.M., C.B. Park, R.D. Miller, and J. Xia, 2000, Mapping Poisson's ratio of unconsolidated materials from a joint analysis of surface-wave and refraction events: Proceedings of the Symposium on the Application of Geophysics to Engineering and Environmental Problems (SAGEEP 2000), Arlington, Va., February 20-24.

Kilty, K.T., and A.L. Lange, 1990, Acoustic tomography in shallow geophysical exploration using a transform reconstruction: Soc. Explor. Geophys. Investigations in Geophysics no. 5, S.H. Ward, ed., *Volume 3: Geotechnical*, p. 23-35.

Knapp, R.W., and D.W. Steeples, 1986, High-resolution common-depth-point, seismic-reflection profiling: Field acquisition parameter design: *Geophysics*, v. 51, p. 283-294.

Lo, T., M.N. Toksoz, S. Xu, and R. Wu, 1988, Ultrasonic laboratory tests of geophysical tomographic reconstruction: *Geophysics*, p. 947-956.

Lytle, R.J., and K.A. Dines, 1980, Iterative ray tracing between boreholes for underground image reconstruction: Inst. Electr. Electron. Eng. Trans. Geosci. Remote Sensing, v. GE-18, p. 234-240.

Mayne, W.H., 1962, Horizontal data stacking techniques: Supplement to *Geophysics*, v. 27, p. 927-938.

Miller, R.D., 1992, Normal moveout stretch mute on shallow-reflection data: *Geophysics*, v. 57, p. 1502-1507.

Miller, R.D., C.B. Park, T.S. Anderson, R.F. Ballard, K. Park, J. Xia, and M.L. Moran, 2002, Wavefield imaging to detect underground facilities: Proceedings of the Military Sensing Symposia Specialty Group on Battlefield Acoustic and Seismic Sensing, September 24-26, Laurel, Maryland, Published on CD.

Miller, R.D., C.B. Park, J.M. Ivanov, J. Xia, D.R. Laflen, and C. Gratton, 2000, MASW to investigate anomalous near-surface materials at the Indian Refinery in Lawrenceville, Illinois: Kansas Geological Survey Open-file Report 2000-4.

Miller, R.D., D.W. Steeples, and M. Brannan, 1989, Mapping a bedrock surface under dry alluvium with shallow seismic reflections: *Geophysics,* v. 54, p. 1528-1534.

Miller, R.D., and D.W. Steeples, 1991, Detecting voids in a 0.6-m coal seam, 7 m deep, using seismic reflection: *Geoexploration,* Elsevier Science Publishers B.V., Amsterdam, The Netherlands, v. 28, p. 109-119.

Miller, R.D., D.W. Steeples, and P.B. Myers, 1990, Shallow seismic-reflection survey across the Meers fault, Oklahoma: *GSA Bulletin*, v. 102, p. 18-25.

Miller, R.D., and J. Xia, 1998, Large near-surface velocity gradients on shallow seismic reflection data: *Geophysics*, v. 63, no. 4, p. 1348-1356.

Miller R.D., and J. Xia, 1999, Using MASW to map bedrock in Olathe, Kansas: Kansas Geological Survey Open-file Report 99-9.

Miller, R.D., J. Xia, and C.B. Park, 1999, MASW to investigate subsidence in the Tampa, Florida area: Kansas Geological Survey Open-file Report 99-33.

Miller, R.D., J. Xia, C.B. Park, and J.M. Ivanov, 1999, Multichannel analysis of surfaces waves to map bedrock: *Leading Edge*, v. 18, n. 12, p. 1392-1396.

Nazarian, S., K.H. Stokoe II, and W.R. Hudson, 1983, Use of spectral analysis of surface waves method for determination of moduli and thicknesses of pavement systems: Transportation Research Record No. 930, p. 38-45.

Park, C.B., R.D. Miller, and J. Ivanov, 2002, Filtering surface waves: Symposium on the Application of Geophysics to Engineering and Environmental Problems (SAGEEP 2002), Las Vegas, Nevada, February 10-13, Paper 12SEI9, published on CD.

Park, C.B., R.D. Miller, D.W. Steeples, and R.A. Black, 1996, Swept impact seismic technique (SIST): *Geophysics*, v. 61, p. 1789-1803.

Park, C.B., R.D. Miller, and J. Xia, 1998, Imaging dispersion curves of surface waves on multi-channel record [Exp. Abs.]: Soc. Expl. Geophys., p. 1377-1380.

Park, C.B. R.D. Miller, and J. Xia, 1999, Multichannel analysis of surface waves (MASW): *Geophysics*, v. 64, p. 800-808.

Peterson, J.E., B.N.P. Paulsson, and T.A. McEvilly, 1985, Applications of algebraic reconstruction techniques to cross-hole data: *Geophysics*, v. 53, p. 1284-1294.

Schepers, R., 1975, A seismic reflection method for solving engineering problems: *Journal of Geophysics*, v. 41, p. 267-284.

Steeples, D.W., and R.D. Miller, 1990, Seismic reflection methods applied to engineering, environmental, and groundwater problems: Soc. Explor. Geophys. Investigations in Geophysics no. 5, Stan H. Ward, ed., *Volume 1: Review and Tutorial,* p. 1-30.

Steeples, D.W., C.M. Schmeissner, and B.K. Macy, 1995, The evolution of shallow seismic methods: *Journal of Environmental and Engineering Geophysics*, v. 0, n. 1, p. 15-24 (invited paper).

Stokoe II, K.H., G.W. Wright, A.B. James, and M.R. Jose, 1994, Characterization of geotechnical sites by SASW method: in *Geophysical Characterization of Sites*, ISSMFE Technical Committee #10, ed. R.D. Woods, Oxford Publishers, New Delhi.

Xia, J., R.D. Miller, and C.B. Park, 1999, Estimation of near-surface velocity by inversion of Rayleigh waves: *Geophysics*, v. 64, p. 691-700.

Xia, J., R.D. Miller, and C.B. Park, 2000, Advantages of calculating shear-wave velocity from surface waves with higher modes: [Exp. Abs.]: Soc. Expl. Geophys., p. 1295-1298.

Yilmaz, O., 1987, Seismic data processing; S.M. Doherty, ed.; *in* Series: Investigations in Geophysics, no. 2, E.B. Neitzel, series ed.: Soc. Explor. Geophys.